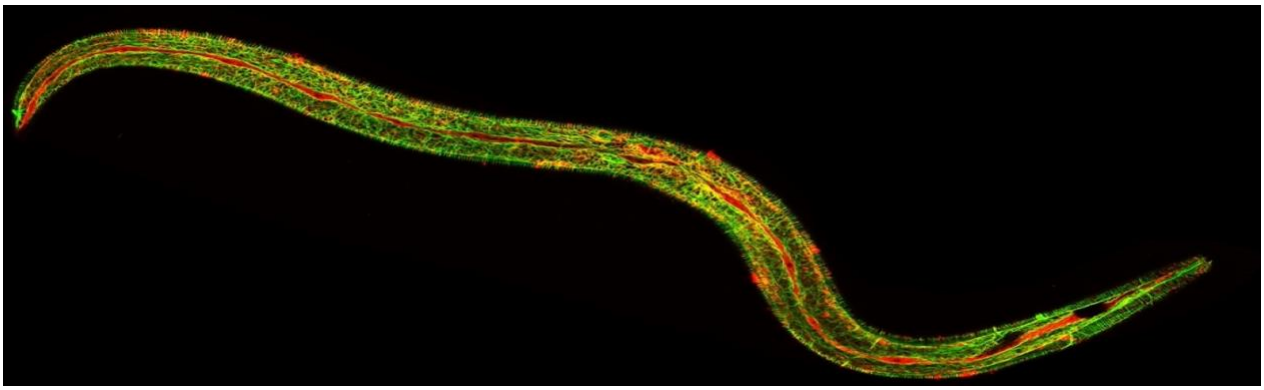

Microtubule (green) and actin (red) cytoskeleton in C. elegans *epidermis. Copyright Sébastien Mailfert & Nathalie Pujol, CIML.*[i]

Model and Simulation of the Pentose Phosphate Pathway in *Caenorhabditis elegans*

Nikki Tirrell, Casey Grage, Libby Lewis

Johns Hopkins University Systems Biology Fall 2022

Professor Christopher Bradburne

November 1st, 2022

ABSTRACT

The nematode worm *Caenorhabditis elegans*, or *C. elegans*, contains many cellular and biological processes that are similar to and simplified from their human counterparts. This reality exists because approximately 38% of *C. elegans'* protein-coding genes have human orthologs despite the adult worm only reaching about 1mm in length in adulthood! Such genes are particularly present in the pentose phosphate pathway. The known scientific knowledge of both the *C. elegans* and human pentose phosphate pathways and the acute similarity of these pathways to each other are two primary reasons we decided to model and simulate the pentose phosphate pathway in *C. elegans*. We wrote ordinary differential equations to create a network-based model for this pathway, making a knowingly inaccurate assumption that 100% of glucose entering the pathway of the organism goes toward this one reaction. Then, we ran time course simulations in both Copasi and CellDesigner in order to vary the amount of time, stochastic vs. deterministic methods, Mass Action vs. Michaelis-Menten kinetic laws, initial concentration values, and the reaction rate values (k_m, v_{max}, and k_1). We found that employing a deterministic continuous model with ordinary differential equations demonstrated the same end behavior trends provided the amount of time run, reaction rate, and initial concentrations were in a proportion to each other such that the asymptote could be reached without concentrations going into negative values. We were able to explain, but not adjust via our software tools, the flaw in our model that the delay in one additional substrate was unaccounted for. Conversely, we were unable to explain at all why three substrates did not reach their expected peak concentration amounts. Hence, we were unsure if this was a flaw in the model or in our interpretation of what the model should produce. Despite these shortcomings, we were able to hypothesize the effects of a particular overexpression in the pathway, and the model proved successful in simulating the results—proving our predictions correct and demonstrating additional logical results which we had failed to anticipate. In conclusion, this model may be a slightly inaccurate but altogether useful tool in predicting variations of the pentose phosphate pathway in *C. elegans*, and therefore, in humans.

BACKGROUND

We chose the nematode *Caenorhabditis elegans*, or *C. Elegans*, to serve as our model. The purpose of a biological model is to create a simplified visualization of a human biological pathway. The multicellular *C. elegans*, via both analogous and homologous structures, is in many ways a simpler and better understood cousin to many molecular and cellular processes in humans. It is evident that *C. elegans'* biological processes are less convoluted than their human equivalents, due to the comparative dearth of organs and size, and therefore more easily understood. For example, *C. elegans* is the only animal in existence for which scientists have constructed its complete nervous system connectome,[ii] [iii] and *C. elegans* was the first multicellular organism for which scientists determined its complete genome sequence.[iv] [v] We know that *C. elegans*' cellular processes are similar to humans because, of the approximately 20,250 to 21,700 predicted protein-coding genes in *C. elegans*,[vi] [vii] about 38% conservatively have human orthologs.[viii] Additionally, scientists have created incredibly detailed anatomical models as a result of the fixed number of somatic cells that are identical in all the individual nematodes: 959 in hermaphrodites and 1031 in males. Databases such as WormBase[ix] or WormBook[x] provide a user interface easily accessible by non-experts which demonstrates anatomical analogies between humans and *C. elegans*.

Of course, since we chose to model the pentose phosphate pathway, we needed to pay special attention to the human orthologs for this particular pathway within *C. elegans*. A few relevant genes with such human orthologs are *DAF-2* which encodes a homolog of a mammalian insulin-like growth factor,[xi] *F07A11.5* — an orthologue of human ribokinase, and *RPB-6* — a gene encoding a human orthologue of RNA polymerase II subunit F.[xii] These genes create a very similar pentose phosphate pathway in *C. elegans* to that of humans. We can directly compare these two pathways via WikiPathways.[xiii] Below, the *C. elegans* pentose phosphate pathway is pictured to the left[xiv] and the equivalent pathway in homo sapiens senescent cells is pictured to the right[xv]:

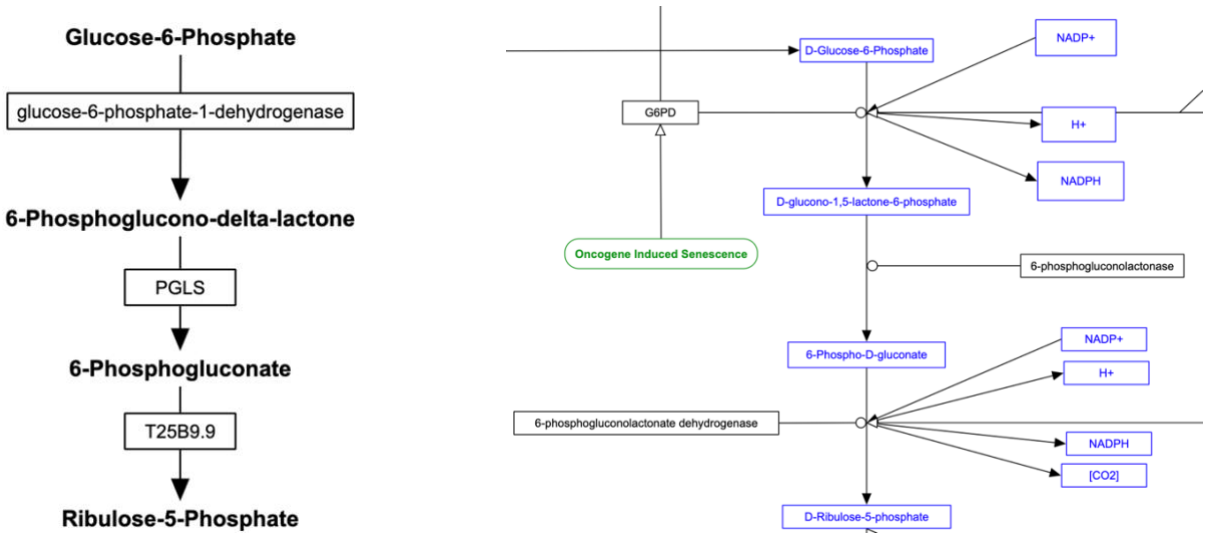

Figure 1a. C. elegans pentose phosphate pathway via WikiPathways (left).

Figure 1b. Human senescent cells pentose phosphate pathway via WikiPathways (right).

As already discussed, and as clearly displayed above, the *homo sapiens* pentose phosphate pathway is certainly more complicated as it features several co-mingled pathways. If, however, we ignore the interconnected pathways and focus solely on the central vertical column, we see it looks very similar to *C. elegans*! The reactions are identical with only slightly differentiated substrates. The enzymes involved are also different from one another though they are not pictured above.

Not directly relevant to this project but still important to note in case this project were to extend to experimental studies are the practical and logistical benefits of experimentation with *C. elegans*. For one, it is a single organism only reaching about 1mm in length at its zenith, so thousands can be kept and maintained with minimal storage space. Its diet consists of easily cultured bacteria or synthetic alternatives, and the majority of *C. elegans* can self-reproduce hermaphroditically. The life cycle of such reproduction only takes approximately 2.5 to 5.5 days, depending on temperature, and each organism's lifespan is approximately two to three weeks. This rapid lifecycle makes *C. elegans* a fantastic model for aging and apoptosis discoveries.[xvi]

APPROACH/RESULTS

In order to develop our model, we followed the 10-step guidelines as outlined in the textbook.[xvii]

Step 1: Define the model

In the first step of this process, we chose the foundation of our model. We picked *C. elegans* as our model organism due to its simplicity and extensive modeling as previously described in the Background section. We considered several processes to model in this system. Option one was the pentose phosphate pathway, option two was apoptosis, and option three was the Entner-Dourdoroff pathway. The question that we wanted to answer was how this process is carried out in *C. elegans*.

Step 2: Literature Review

After choosing these three options for pathways to model, we conducted a thorough literature search in order to determine which option had the most reliable information.

We found several experimental articles on the pentose phosphate pathway in *C. elegans*, as well as the detailed pathway in relevant databases: WikiPathways,[xviii] Reactome,[xix] and KEGG.[xx]

Literature:

→ Arwen W. Gao, Reuben L. Smith, Michel van Weeghel, Rashmi Kamble, Georges E. Janssens, Riekelt H. Houtkooper, Identification of key pathways and metabolic fingerprints of longevity in C. elegans, Experimental Gerontology, Volume 113, 2018, Pages 128-140, ISSN 0531-5565, https://doi.org/10.1016/j.exger.2018.10.003. https://www.sciencedirect.com/science/article/pii/S0531556518301141 [xxi]

- Annotation: Detailed description of pentose phosphate pathway in *C. elegans.*

Databases:

→ https://www.wikipathways.org/index.php/Pathway:WP312 xv

- Annotation: *C. Elegans* pentose phosphate pathway nodes modelled.

→ http://reactome.org/content/detail/R-CEL-71336 [xxii]

- Annotation: *C. Elegans* pentose phosphate pathway nodes modelled.

→ https://www.genome.jp/pathway/cel00030+M00006 [xxiii]

- Annotation: *C. Elegans* pentose phosphate pathway nodes modelled.

We also found published articles about the apoptosis pathway in C. elegans with limited pathway information. The enzymes involved in this process were shown in pathway databases WikiPathways,[xxiv] Reactome,xix and KEGG.xx

Literature:

→ van den Heuvel S. The *C. elegans* cell cycle: overview of molecules and mechanisms. Methods Mol Biol. 2005;296:51-67. PMID: 15576926. https://pubmed.ncbi.nlm.nih.gov/15576926/, [xviii]

- Annotation: General overview of several pathways within *C. elegans* including apoptosis.

→ Genetics 14: 'C. Elegans methods workshop' or, 'Putting genes into path- ways' (cureffi.org), http://www.cureffi.org/2014/10/20/genetics-14/ [xix]

- Annotation: A literature review about apoptosis pathway in *C. elegans* conducted by a student. Not a first-hand source but a useful compilation for future reference.

→ Schleich, K., Lavrik, I.N. Mathematical modeling of apoptosis. *Cell Commun Signal* **11**, 44 (2013). https://doi.org/10.1186/1478-811X-11-44. , https://biosignaling.biomedcentral.com/articles/10.1186/1478-811X-11-44 [xx]

- Annotation: Mathematical modelling of apoptosis in humans.

→ Thomas Eissing, Holger Conzelmann, Ernst D. Gilles, Frank Allgöwer, Eric Bullinger, Peter Scheurich, Bistability Analyses of a Caspase Activation Model for Receptor-induced Apoptosis*, Journal of Biological Chemistry, Volume 279, Issue 35, 2004, Pages 36892-36897, ISSN 0021-9258, https://doi.org/10.1074/jbc.M404893200. https://www.sciencedirect.com/science/article/pii/S0021925820859419 [xxi]

- Annotation: Mathematical modeling and simulation of apoptosis pathway in humans, including ordinary differential equations.

→ Programmed cell death - WormBook - NCBI Bookshelf (nih.gov): https://www.ncbi.nlm.nih.gov/books/NBK19668/ [xxii]

- Annotation: Detailed description of apoptosis pathway in *C. elegans.*

Databases:

- → Programmed cell death and cell engulfment (Caenorhabditis elegans) - WikiPathways: https://www.wikipathways.org/index.php/Pathway:WP2829, [xxiii]
  - Annotation: *C. Elegans* apoptosis pathway nodes modelled.
- → Reactome — Intrinsic Pathway for Apoptosis: https://reactome.org/content/detail/R-CEL-109581 [xxiv]
  - Annotation: *C. Elegans* apoptosis pathway nodes modelled.
- → KEGG PATHWAY: cel04215 https://www.kegg.jp/entry/cel04215 [xxv]
  - Annotation: *C. Elegans* apoptosis pathway nodes modelled.

After finding enough information for options one and two, we found fewer articles on option three. Thus, we decided not to move forward with the Entner-Dourderoff pathway.

Step 3: Visualize the model

We organized the information gathered in the Literature Review section to create a node model of each pathway. We chose this network-based model to visualize the pathway because network descriptions were more readily available in literature and in databases than any set of rules to inform a rule-based network. The pathway databases served as primary reference for this section. We chose to conceptualize the pathways as we would input them into the simulation software Copasi or CellDesigner, and therefore organized them in terms of their species and reactions.

Option one, the pentose phosphate pathway, has seven species: glucose-6-phosphate (abbreviated to “G-6-P"), 6-phosphoglucono-delta-lactone, 6-phosphogluconate, ribulose 5-phosphate, CO2, NADP+, and NADPH. This pathway is shown in Figure 2 below.

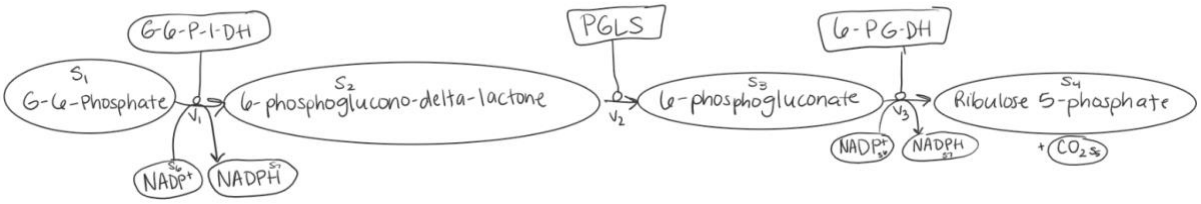

Figure 2. Pentose Phosphate Pathway in C. elegans.

Option two, the apoptosis pathway, has four species, which are the enzymes: EGL-1, CED-9, CED-4, and CED-3. This process, shown below in Figure 3, begins with EGL-1 protein being activated in cells that will die. EGL-1 then binds to and inhibits CED-9, which stops CED-9 from inhibiting CED-4. This activates CED-4, enabling CED-4 to activate CED-3. CED-3 is a caspase, which then causes cell death. This pathway stands out from option one, since it only includes enzymes that are not consumed in a reaction. However, this is the pathway that is shown in the pathway databases and literature, so there is no other data available to include species in the reaction that would be consumed! While this made option two a less viable option, it was still an exciting possibility for this Discovery Project.

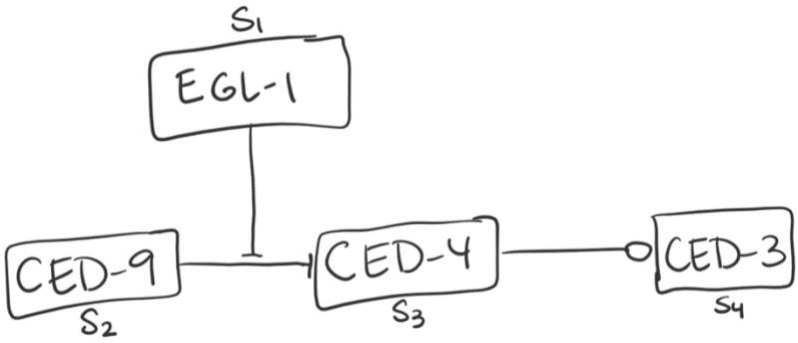

Figure 3. Apoptosis Pathway in C. elegans.

We decided to create a preliminary model of *C. elegans* apoptosis in CellDesigner to determine the viability of modeling this pathway in the software available to us. As feared, CellDesigner would not allow for enzymes or proteins to be modeled as reacting with one another, as shown in the WikiPathways network model. This failed attempt is displayed in Figure 4. In fact, the software only allowed the proteins to interact with the reaction between two of the same protein. For example, EGL-1 is shown to inhibit CED-9 to CED-9. The proteins needed to be identical, which proved a confusing and inaccurate visualization of the pathway.

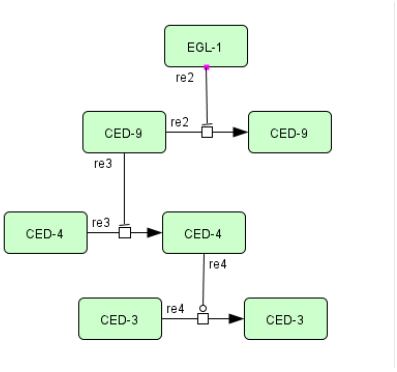

Figure 4. CellDesigner pathway of apoptosis.

Step 4: Conceptualize the model

We then needed to categorize whether our model would be network-based, rule-based, or statistics-based. Since we were not analyzing a large pool of data, or any real data for that matter, we eliminated 'statistics-based' as a potential model. Next, the Literature Review provided clear networks to guide this pathway but only a loose set of theories for rules guiding this pathway. We created the structural/qualitative model of network graphs in Step 3 from this available data. Therefore, we decided to create a **network-based model**, rather than rule-based.

To test and learn from our model, we decided we would run time course simulations of substrate concentrations, because substrate concentrations are the most dynamic variable, the substrate concentrations vary primarily based on time, the results could be measured against our predictions, and because this simulation was easily accessible to us in our available software: Copasi and CellDesigner. The use of the independent variable time definitionally makes this model dynamic. To run such time course simulations, we knew we would need to create a new network-based quantitative model by assigning values, temporary or otherwise, to the substrates and their interactions. Our independent x-axis variable, time, would be measured continuously rather than in discrete periods. Hence, we decided to create a **continuous network-based dynamic quantitative model.** We then needed to decide whether our network-based model would be Stochastic, Boolean, Statistic, or Deterministic.

Stochastic models are typically used when not enough information is available to construct deterministic models because they create a probability distribution of potential future states. Since stochastic simulations are usually more expensive to perform, they should only be used when random fluctuations matter. Such random fluctuations matter more within smaller amounts of particles in the system.[xix] In running a time course simulation of a stochastic model, we would compare our experimentally calculated probabilities with those of our predictions. One downside of the stochastic model is that predicting probability is much more difficult to do via Fermi estimation.

Boolean models and Petri nets are used for gene regulation because gene expression is a binary of either expressed or not expressed. This type of model was therefore not as relevant to either the apoptosis or pentose phosphate pathways as a model based on continuous time would be.[xix]

However, we did attempt a Petri net model to look at discrete time steps of the pentose phosphate pathway, which we have included in the Supplemental Materials section since it did not pertain to the main portion of our research.

Deterministic models need to contain enough information to predict the behavior of a given system for all future times. For example, in kinetic rate equation models, the given state is a list of substance concentrations and future states are determined by the current state. Deterministic kinetic modeling of individual biochemical reactions is typically used in enzymatic reactions.[xix] In our model testing, we would compare predicted values with experimentally calculated values. One benefit of the deterministic model is that predicting values via Fermi estimation is relatively straightforward, making the results easier to analyze.

For both the apoptosis and pentose phosphate pathways, we could assume large concentrations of initial substrates which are therefore largely unaffected by random fluctuations. As far as available information, we did have a large range of acceptable given initial concentrations for the pentose phosphate pathway from the literature, but we did not have this information for the apoptosis pathway. Additionally, we did not have known values for the given reaction rates of either pathway. The question for both pathways was therefore whether we should make assumptions about the reaction rates and the initial concentrations (within an acceptable range for pentose phosphate) in order to compare deterministic results more easily, or if we should compare stochastic results in order to limit the number of assumptions made.

We decided to employ a **deterministic continuous dynamic quantitative model** for option 1 pentose phosphate pathway, because we had an acceptable range of initial substrate concentrations, could assume large initial concentrations comparatively undistributed by random perturbations, and because the results would be easier to analyze, despite needing to make key assumptions about the reaction rates.

Conversely, we decided to use a **stochastic continuous dynamic quantitative model** for option 2 apoptosis pathway to avoid making assumptions about initial substrate concentrations and reaction rates, although the results would be more difficult to analyze than a deterministic model would have been. With a stochastic model, we could also test both small and large initial substrate concentrations because the effects of random fluctuations would be accounted for.

Step 5: Form A Mathematical Model

After conceptualizing the models, we defined them mathematically and related them to one another using ordinary differential equations "ODEs" with respect to time. We chose this method because ODE systems relate substrates to one another in a straightforward fashion and account for continuous, rather than discrete, time. First, we defined the reactions, and then we wrote the differential equations to describe the reactions. The equations for the option 1 pentose phosphate pathway are shown in Equations 1 through 3 below, and the ordinary differential equations for option 1 are shown in Equations 4 through 10 below. The species designations are referenced from Figure 2.

1) Pentose phosphate pathway reaction 1: $v_1 = k_1 S_1 S_6$
2) Pentose phosphate pathway reaction 2: $v_2 = k_2 S_2 S_7$
3) Pentose phosphate pathway reaction 3: $v_3 = k_3 S_3 S_6$
4) Ordinary differential equation "ODE" for glucose-6-phosphate: $\frac{dS_1}{dt} = -v_1 = -k_1 S_1 S_6$
5) ODE for 6-phosphoglucono-delta-lactone: $\frac{dS_2}{dt} = v_1 - v_2 = k_1 S_1 S_6 - k_2 S_2 S_7$
6) ODE for 6-phosphogluconate: $\frac{dS_3}{dt} = v_2 - v_3 = k_2 S_2 S_7 - k_3 S_3 S_6$
7) ODE for ribulose-5-phosphate: $\frac{dS_4}{dt} = v_3 = k_3 S_3 S_6$
8) ODE for CO2: $\frac{dS_5}{dt} = v_3 = k_3 S_3 S_6$
9) ODE for NADP+: $\frac{dS_6}{dt} = -v_1 - v_3 = -k_1 S_1 S_6 - k_3 S_3 S_6$
10) ODE for NADPH: $\frac{dS_7}{dt} = v_1 + v_3 = k_1 S_1 S_6 + k_3 S_3 S_6$

The equations for option two apoptosis are shown in Equations 11 through 14 below, and the differential equations are shown in Equations 15 through 18 below. The species designations are referenced from Figure 3. We were able to create potential differential equations for the pathway by assuming that the enzymes are proteins which are consumed in the reaction.

11) Apoptosis pathway reaction 1: $v_1 = k_1 \cdot \{EGL - 1\}$

12) Apoptosis pathway reaction 2: $v_2 = k_2 \cdot \{CED - 9\}$

13) Apoptosis pathway reaction 3: $v_3 = k_3 \cdot \{CED - 4\}$

14) Apoptosis pathway reaction 4: $v_4 = k_4 \cdot \{CED - 3\}$

15) ODE for EGL-1: $\frac{dS_1}{dt} = -v_1 = -k_1 \cdot \{EGL - 1\}$

16) ODE for CED-9: $\frac{dS_2}{dt} = v_2 - v_1 = k_2 \cdot \{CED - 9\} - k_1 \cdot \{EGL - 1\}$

17) ODE for CED-4: $\frac{dS_3}{dt} = v_3 - v_2 = k_3 \cdot \{CED - 4\} - k_2 \cdot \{CED - 9\}$

18) ODE for CED-3: $\frac{dS_4}{dt} = v_3 = k_3 \cdot \{CED - 4\}$

Despite being able to mathematically apoptosis model in option 2, we decided not to move forward with option 2, since the software implementation was proving difficult. It was important to have the correct model in Copasi or CellDesigner in order to accurately simulate the system.

So, we chose **option 1** to move forward!

Step 6: Test the model

Now we needed to test our chosen model against known data. After the comprehensive literature review in Section 2, there appeared to be a dearth of available data on the pentose phosphate pathway in *C. elegans*. Thus, we would need to rely on Fermi estimation modeled after what we had done with upper glycolysis in this course to date, as well as available information about glycolysis in *C. elegans*. Glycolysis is intricately related to the pentose phosphate pathway since the initial species in the pentose phosphate pathway is made during the glycolysis pathway.

A further literature review on glycolysis modeling in *C. elegans*, revealed an NIH article, "*C. elegans* as Model for the Study of High Glucose–Mediated Life Span Reduction",[xxvi] which discusses intracellular concentration of glucose in *C. elegans*. The authors found the intracellular concentration of glucose in *C. elegans* to be 14mmol/L when *C. elegans* was cultured on agar plates with 40mmol/L of glucose.

For our own model, we chose to assume that in glycolysis there is a 1:1 ration of glucose to glucose−6−phosphate "G-6-P". Therefore, we set our starting amount of G-6-phosphate to 14 mM. One key assumption we made was that 100% of the glucose entering the pathway in this nematode went to this one reaction, which is of course not a reasonable assumption. However, we assumed this for the sake of the model and address the possible effects of this assumption in our discussion.

Before modeling the pathway in the simulation software, we manually created time course simulations. Since we did not have experimental data to compare with our results, we decided to use our graphs to guide our analysis. Our time course simulation is shown in Figure 5. Since there are several species to track, we also separated this graph into individual graphs per species for easier visualization (Figure 6).

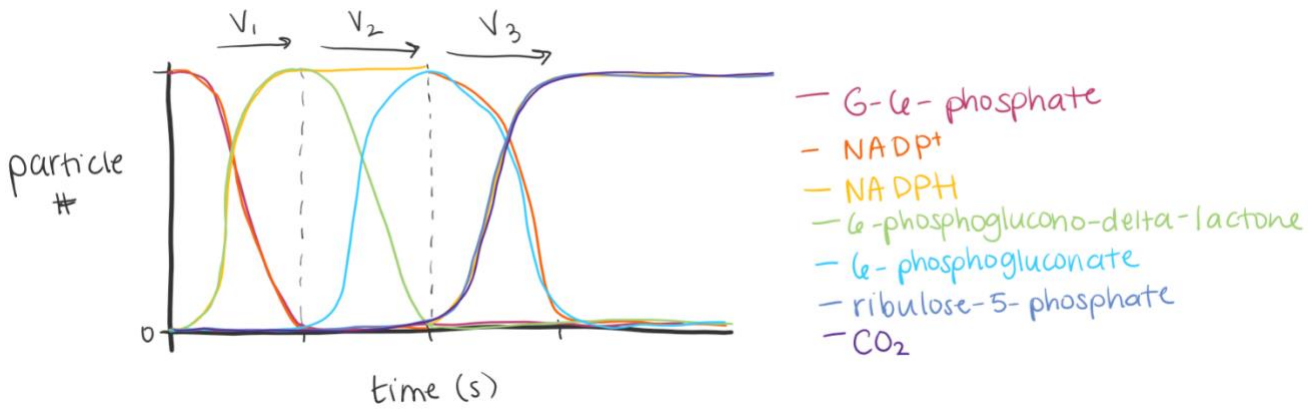

Figure 5. Overall Expected Time Course Simulation.

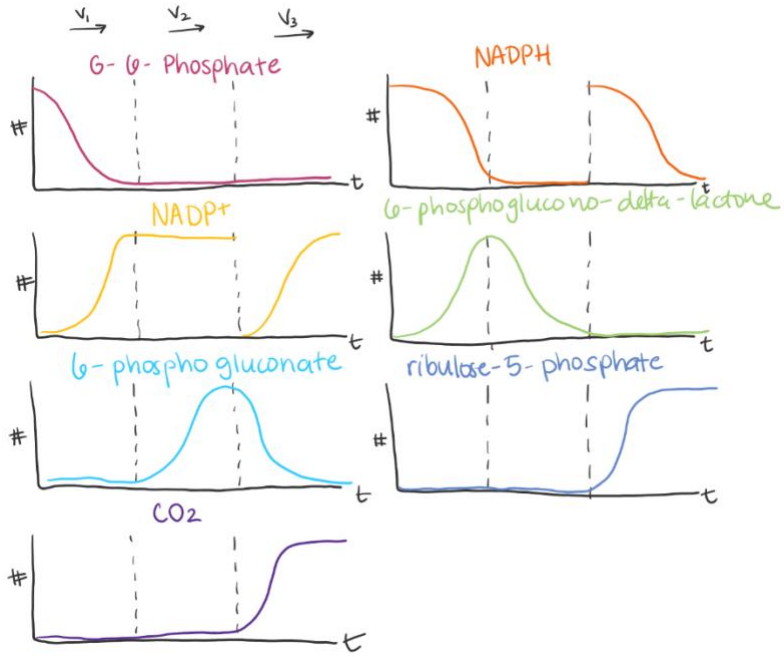

Figure 6. Separate Expected Time Course Simulations for Each Species.

We chose Copasi and CellDesigner as our simulation software to generate time course simulations due to their being free, quick to learn, and easy to manipulate. We started with Copasi and entered the reactions into Copasi as shown in Equations 19 through 21 below.

19) Pentose phosphate pathway reaction 1:

$$v_1: \{G-6-P\} + \{NADP+\} \rightarrow \{6-P-G-delta-lactone\} + \{NADPH\}$$

20) Pentose phosphate pathway reaction 2:

$$v_2: \{6-P-G-delta-lactone\} \rightarrow \{6-phosphogluconate\}$$

21) Pentose phosphate pathway reaction 3:

$$v_3: \{6-phosphogluconate\} + \{NADP+\} \rightarrow \{ribulose-5-phosphate\} + \{CO_2\} + \{NADPH\}$$

We originally thought that Michaelis-Menten kinetics would be the most proper rate laws to employ given the fact that there are enzymes involved. However, the Michaelis-Menten equation does not allow for multiple reactant species, which is the case in Reactions 1 and 3. Due to this limitation, we reasoned that Mass Action kinetics are more appropriate given there are multiple substrates. Additionally, Copasi only offered three options for the rate laws of Reactions 1 and 3 with multiple substrates: irreversible mass action, irreversible Bi, and irreversible constant flux. Thus, we chose Mass Action kinetics for all three reactions to standardize the kinetics.

We used the default reaction rate $k_1 = 0.1$ and the default initial concentrations of NADP+ = 1 mol, G−6−P = 1 mol, and set all other substrates equal to 0 mol. The parameter overview is shown below in Figure 7.

Model Parameters

Name	Type	Value	Unit
Initial Time			
New M...	time	0	s
Initial Com...			
compar...	fixed	1	l
Initial Speci...			
6-P-G-d...	reactions	0	mol/l
G-6-P	reactions	1	mol/l
6-phosp...	reactions	0	mol/l
CO2	reactions	0	mol/l
NADP+	reactions	1	mol/l
NADPH	reactions	0	mol/l
ribulose...	reactions	0	mol/l
Initial Globa...			
Kinetic Para...			
v1			mol/(l*s)
k1	fixed	0.1	l/(mol*s)
v2			mol/(l*s)
k1	fixed	0.1	1/s
v3			mol/(l*s)
k1	fixed	0.1	l/(mol*s)

Figure 7. Copasi Parameter Overview.

Before running the simulation, we confirmed that our differential equations were accurate by checking the differential equations that Copasi created. These are shown in Figure 8.

$$\frac{d(["6\text{-P-G-delta-lactone}"] \cdot V_{compartment})}{dt} = +V_{compartment} \cdot (k1_{(v1)} \cdot ["G\text{-6-P}"] \cdot ["NADP+"]) - V_{compartment} \cdot (k1_{(v2)} \cdot ["6\text{-P-G-delta-lactone}"])$$

$$\frac{d(["G\text{-6-P}"] \cdot V_{compartment})}{dt} = -V_{compartment} \cdot (k1_{(v1)} \cdot ["G\text{-6-P}"] \cdot ["NADP+"])$$

$$\frac{d(["6\text{-phosphogluconate}"] \cdot V_{compartment})}{dt} = +V_{compartment} \cdot (k1_{(v2)} \cdot ["6\text{-P-G-delta-lactone}"]) - V_{compartment} \cdot (k1_{(v3)} \cdot ["6\text{-phosphogluconate}"] \cdot ["NADP+"])$$

$$\frac{d([CO2] \cdot V_{compartment})}{dt} = +V_{compartment} \cdot (k1_{(v3)} \cdot ["6\text{-phosphogluconate}"] \cdot ["NADP+"])$$

$$\frac{d(["NADP+"] \cdot V_{compartment})}{dt} = -V_{compartment} \cdot (k1_{(v1)} \cdot ["G\text{-6-P}"] \cdot ["NADP+"]) - V_{compartment} \cdot (k1_{(v3)} \cdot ["6\text{-phosphogluconate}"] \cdot ["NADP+"])$$

$$\frac{d([NADPH] \cdot V_{compartment})}{dt} = +V_{compartment} \cdot (k1_{(v1)} \cdot ["G\text{-6-P}"] \cdot ["NADP+"]) + V_{compartment} \cdot (k1_{(v3)} \cdot ["6\text{-phosphogluconate}"] \cdot ["NADP+"])$$

$$\frac{d(["ribulose\text{-}5\text{-}phosphate"] \cdot V_{compartment})}{dt} = +V_{compartment} \cdot (k1_{(v3)} \cdot ["6\text{-phosphogluconate}"] \cdot ["NADP+"])$$

Figure 8. Copasi Differential Equations of the system.

To simulate the model, we ran a time course simulation which shows the change in concentration of each species as the pathway progresses. As explained in Step 4, we used the deterministic method. To make sure that we had chosen the right method, we tried a stochastic method as well.

However, the resulting graph showed constant concentrations over time, which we knew to be incorrect. Thus, we validated our decision to use the deterministic method. We started the simulation with an initial concentration of 1 mol of G-6-P and NADP+ to keep values simple and to easily visualize the system. The resulting time course simulation is shown in Figure 9.

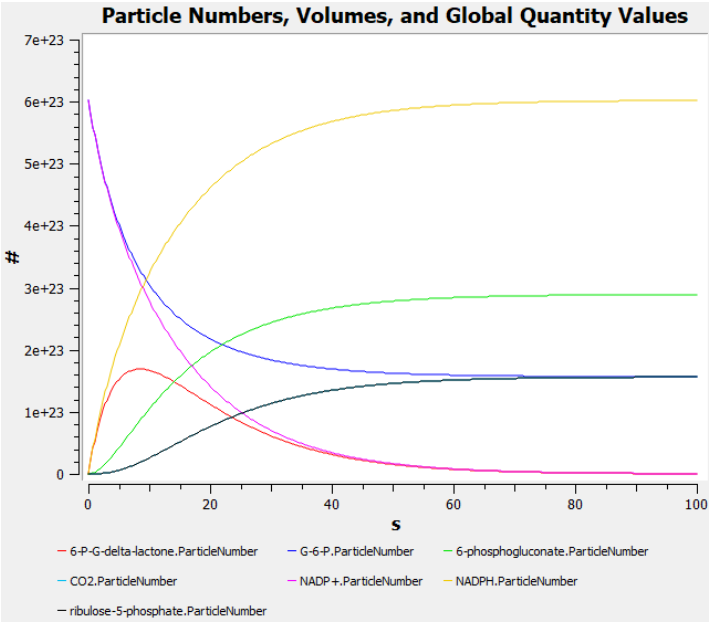

Figure 9. Copasi Time Course Simulation.

This simulation showed some expected and some unexpected results as compared to the graphs in Figures 5 and 6. While our starting species G-6-P decreased in concentration as it was consumed (as predicted), it did not however reduce to 0 mol. This result was unexpected and suggested that G-6-P was not exhausted in the reaction. NADP+ was exhausted in the system as expected. Unexpectedly, NADPH was produced in Reaction 1 but not in Reaction 3. In fact, NADP+ and NADPH did not reflect the addition of NADP+ during Reaction 3 whatsoever. This is a known limitation of Copasi in which species cannot be added on a delay. The amount of NADPH at the end of the pathway is shown to be two, which is a correct result in an ideal environment such as ours as there is a net amount of two NADPH after these reactions, despite its path to get there likely being inaccurate. 6-P-G-delta-lactone is made and then consumed which was expected, however it did not reach the same maximum concentration as G-6-P which was not expected! 6-phosphogluconate was produced, as expected, but not consumed, which was unexpected. Ribulose-5-phosphate and CO2 had the same curve since they were made in the same 1:1 ratio of

the same reaction, which was expected, but as with the other resulting glucose-related species, they did not reach 14 mmol concentration as we had predicted. This is contrary to our belief that the glucose-related species should all be made to the same amount given our preset 1:1:1 ratio of reactants and products in the pathway. To account for the limitations in Copasi which may be causing these unintended effects, we then uploaded the pathway into CellDesigner and created the following reaction:

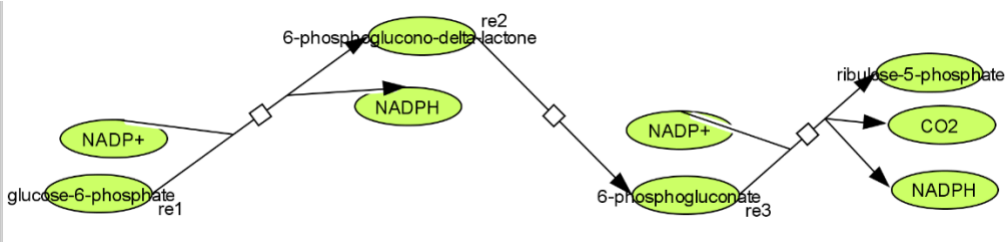

Figure 10. CellDesigner Pentose Phosphate Pathway.

With the change in software, we were able to set the rate laws of these reactions to Michaelis-Menten rather than Mass Action. However, these equations only accounted for one species, and therefore, only accounted for the change in glucose-related species—not in NADP+. We still modelled this pathway to see if the behavior would be different with the change in rate law. The inputted Michaelis-Menten rate laws are shown in Equations 22 through 24 below.

22) Michaelis Menten Equation for reaction 1: $v_1 = \frac{v_{max} S_1}{k_m + S_1}$

23) Michaelis Menten Equation for reaction 2: $v_2 = \frac{v_{max} S_2}{k_m + S_2}$

24) Michaelis Menten Equation for reaction 3: $v_3 = \frac{v_{max} S_3}{k_m + S_3}$

We arbitrarily set $k_m = 2$ and $v_{max} = 5$ because these are standard values as used in the course textbook. The initial concentrations of glucose-6-phosphate and NADP+ were set to 14 mmol, as we found a literature reference indicating that the concentration of glucose-6-phosphate is 14 mmol in *C. elegans*. This assumption and change to our model will be further explored in the discussion. This change resulted in the time course simulation shown below in Figure 11.

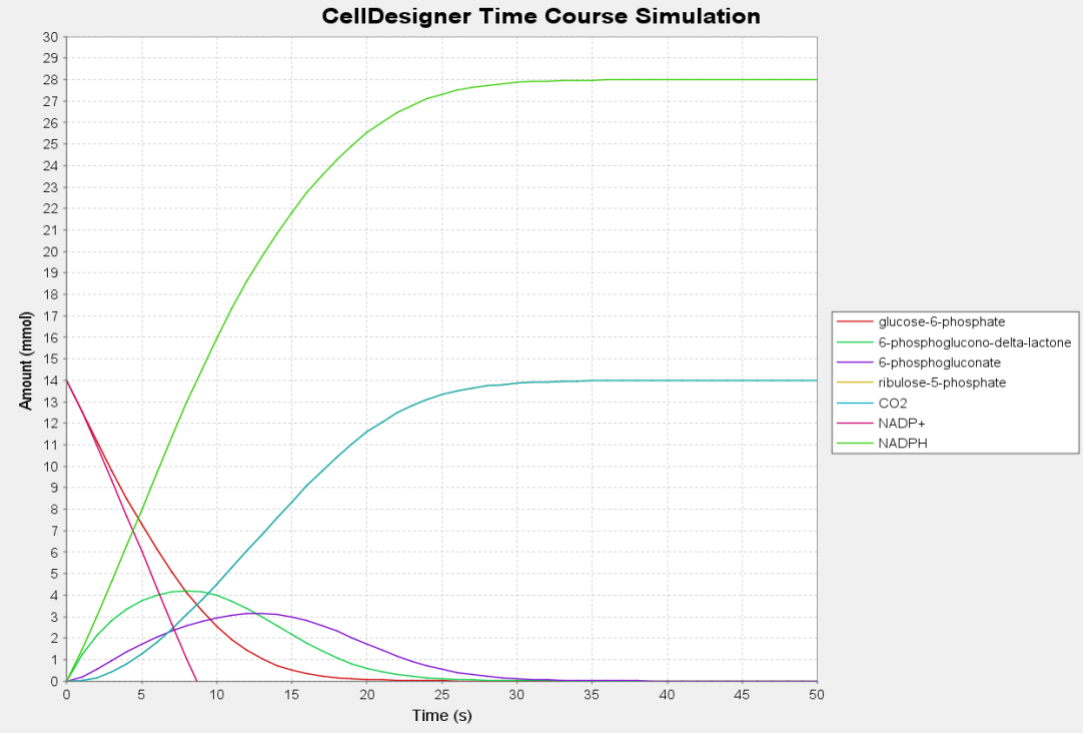

Figure 11. CellDesigner Time Course Simulation.

Interestingly, this time course graph looks incredibly similar to the Copasi results even with the kinetic laws changed to Michaelis-Menten! The primary difference is that 6-phospholuconate is consumed and simply that the reaction occurs faster, which makes sense given the higher arbitrary values of reaction rates we set.

An unexpected result in this simulation is that the amounts of 6-phosphoglucono-delta-lactone and 6-phosphogluconate are less than 14 mmol. In an ideal case, Reaction 1 would result in the same final concentration of 6-phosphoglucono-delta-lactone as the initial concentration of glucose-6-phosphate as would Reaction 3 result in the same final concentration of 6-phosphogluconate. One theory as to why this discrepancy occurred is that the simulation accounts for nonideal conditions. It would make sense in a nonideal case that 6-phosphogluconate has a lower concentration than 6-phosphoglucono-delta-lactone because it is made in a later reaction. If CellDesigner is indeed accounting for nonideal conditions, then the parameters it is utilizing to do so are purely interior and immutable by users. We will analyze this theory further in Step 7.

Step 7: Refine the model

To refine our Copasi model, we doubled the initial concentration of NADP+ to 2 mol. We realized that there are two units of NADP+ entering the pathway—one at Reaction 1, and one at Reaction 3. One issue with the previous graph was that it did not account for this second addition of NADP+ nor subsequent creation of NADPH. Adjusting the initial concentration to 2 mol was an attempt to correct this. However, being unable to delay the addition of the second NADP+, we were unsure if the program would set one NADP+ to go into v_1 and one to go into v_3. We ran this time course simulation below in Figure 12:

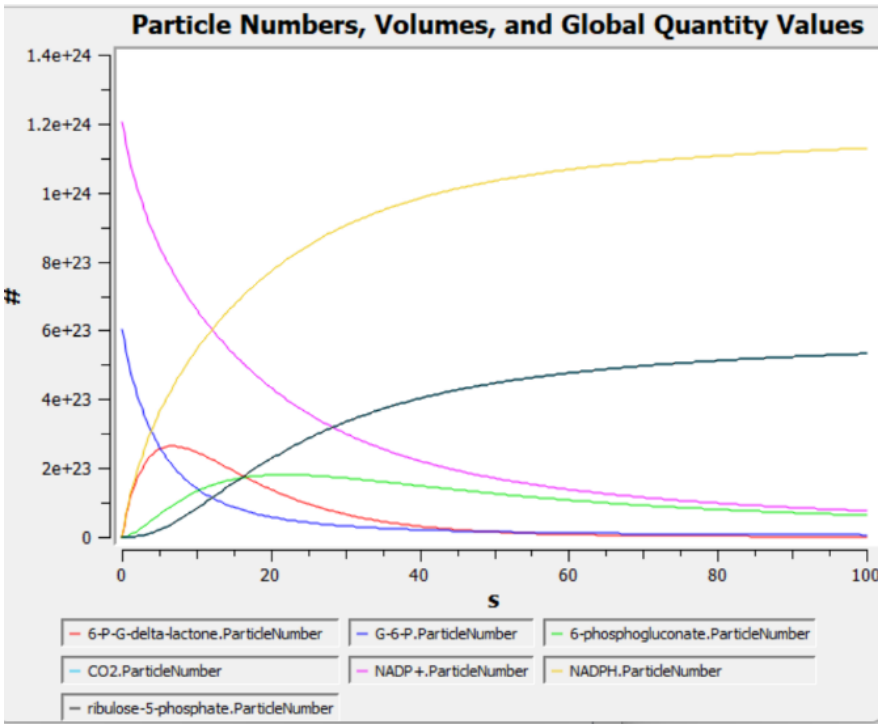

Figure 12. Copasi Time Course Simulation with Doubled NADP+ Initial Concentration.

Figure 12 yielded very similar results to before, demonstrating that our attempt to model the delay likely failed.

In order to determine the end behavior of the system, we set the simulation to 1,000 seconds instead of 100. This would confirm if species such as G-6-P were indeed exhausted after all, though just over a longer period of time than we initially expected.

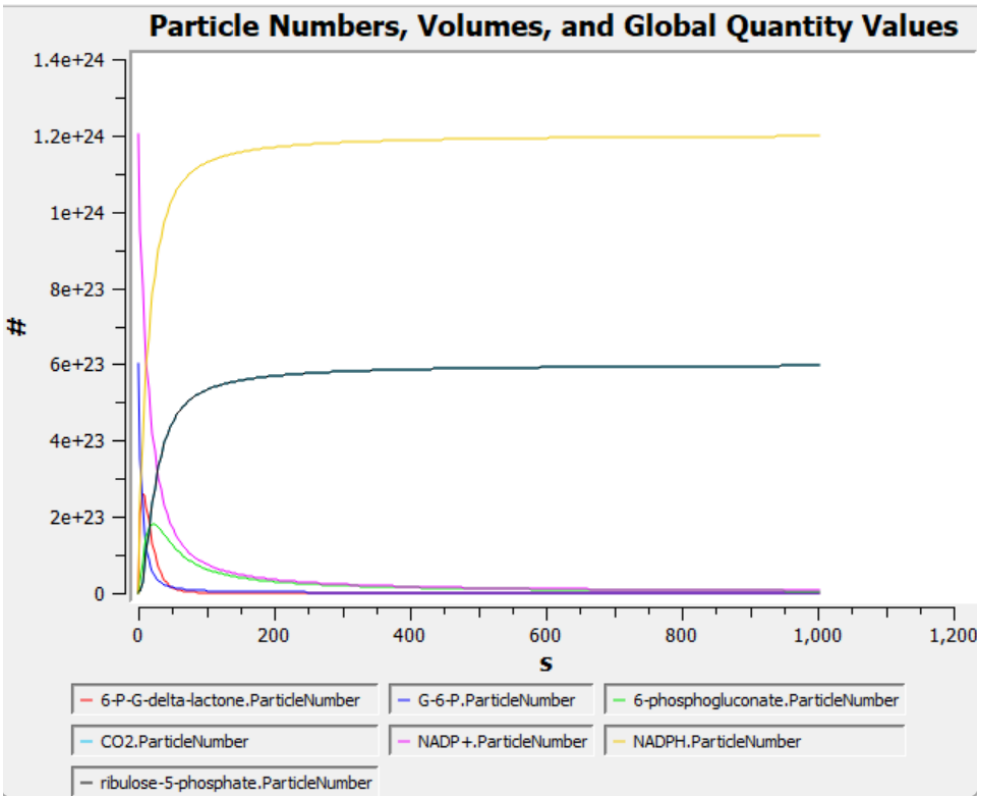

Figure 13. Copasi Extended Time Course Simulation.

Figure 13 shows that this was indeed the case! All the species we predicted would be exhausted do get completely consumed, just over a longer time span than we predicted. It is possible that Copasi runs each time step with the entire set of differential equations, rather than each time step as a step in the reaction. If this is the case, then it made sense that 2 NADP+ were needed right away in order to complete the full pathway. Plus, when we used 2 NADP+, 6-phosphogluconate appeared to be exhausted as well. Perhaps in our first model, the 6-phosphogluconate was not consumed as a result of there not being a second NADP+ present to perform the reaction. One hole in this theory is that ribulose-5-phosphate and CO_2 were also made. If this theory were correct and there was no NADP+ left to perform the reaction from 6-phosphogluconate to ribulose 5-phosphate, then there should have been little to no ribulose-5-phosphate or CO2 being formed. However, since there was still a significant amount of ribulose 5-phosphate formed with only 1 mol NADP+, this theory does not quite hold. However, there is also almost double the amount or ribulose-5-phosphate formed and all the 6-phosphogluconate is consumed in the model with 2 mol

NADP+, so it does seem that there is some correlation between the amount of NADP+ and the ability of the reaction from 6-phosphogluconate to ribulose-5-phosphate to occur.

Once we found literature referencing a potential initial concentration of G-6-P as 14 mmol, we changed our simulation to reflect this information. Replacing a key assumption with an educated estimate made the model more accurate. We also changed the initial concentration of NADP+ to 28 mmol (double the concentration of G-6-P) to reflect this finding. We did not expect this to change the simulation, since every species was still in the same ratio, but it did (Figure 14)! The reaction occurred quicker, with the end behavior visible within the 100s window. This also resulted in steeper changes in concentration.

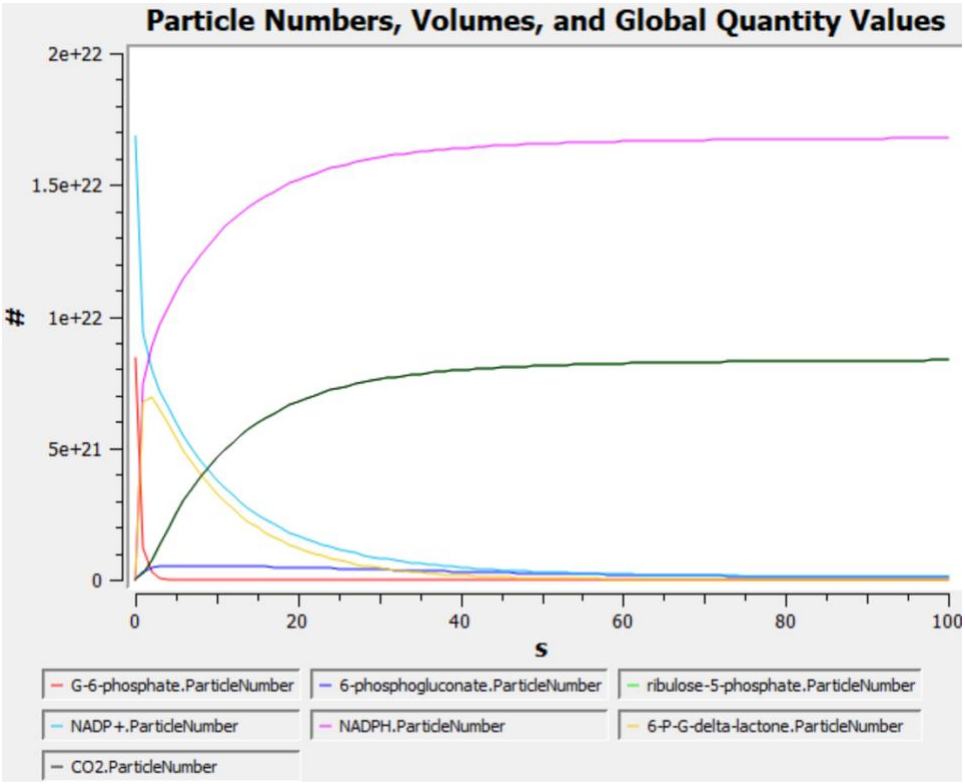

Figure 14. Copasi Time Course Simulation with Initial Concentration of 14 mmol.

Step 8: Analyze the system

Once we had an idea of the model performance, we analyzed the model further by changing certain parameters. In CellDesigner, we varied the Michaelis-Menten kinetic rate variables k_m and v_{max}, and in Copasi, we varied the Mass Action kinetic rate variable k_1 for each reaction.

First, we set $k_m = 1$ and $v_{max} = 1$. The initial concentrations were the same as the first graph. However, running this simulation resulted in a negative concentration of NADP+ since two units were consumed in the pathway. We then created Figure 15 by changing the initial concentration of NADP+ to 28 mmol.

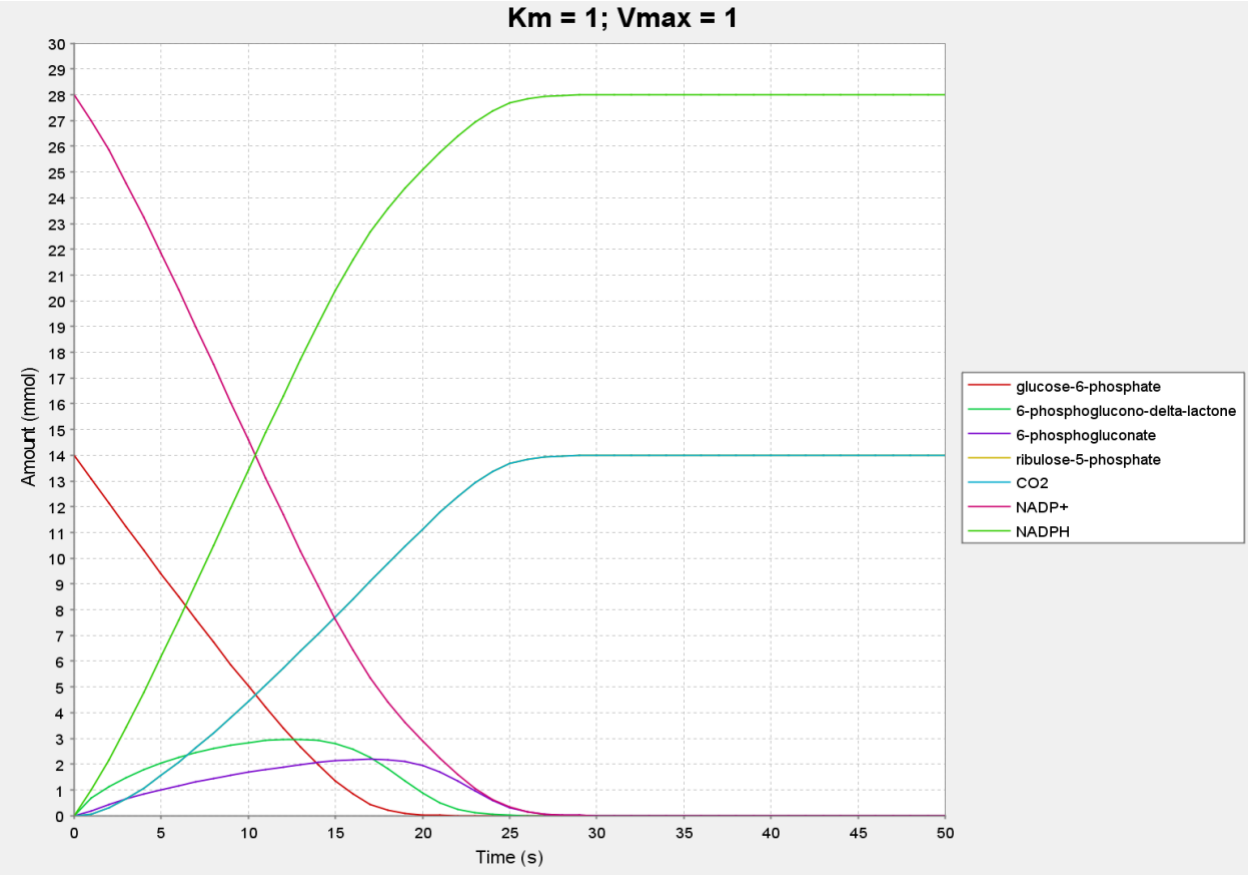

Figure 15. CellDesigner Time Course Simulation with Changed Parameters.

The end behavior was accurate, and the general behavior of the graph was congruent to the original conditions. The most noticeable difference was that 6-phosphoglucono-delta-lactone and 6-phosphogluconate were produced in even lower concentrations.

We changed these conditions one more time to determine further trends. We set k_m=5 and v_{max}=2, to reverse the initial conditions. This created the result in Figure 16.

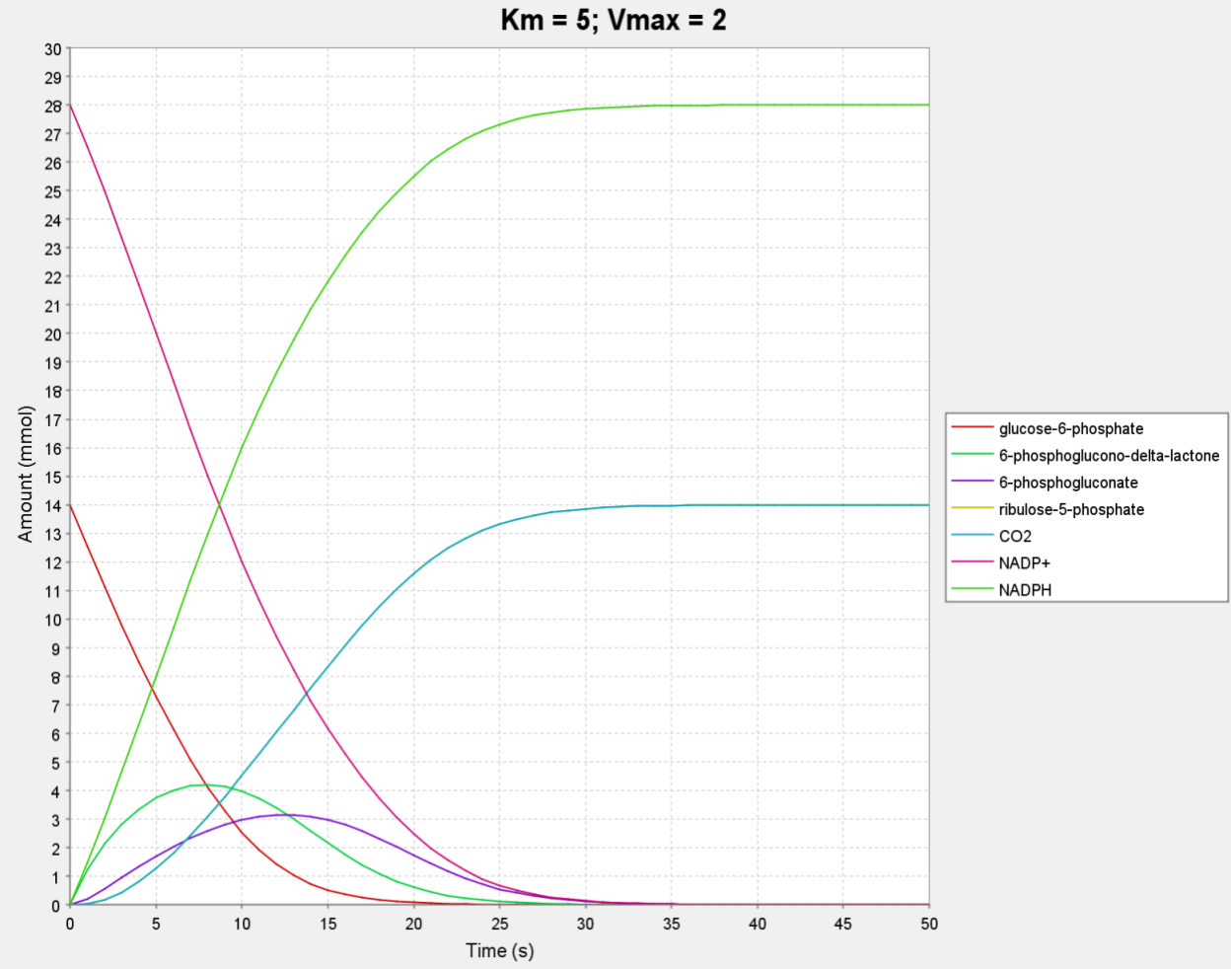

Figure 16. Second CellDesigner Time Course Simulation with Changed Parameters.

The simulation reached asymptotic steady state at about the same time as the previous simulation. There was a slightly larger amount of 6-phosphoglucono-delta-lactone and 6-phosphogluconate made than in the previous simulation, but the end behavior remained the same.

Then, we analyzed the change in Copasi when we varied the k values, especially as they related to each other for each reaction. Initially, the k value for each reaction was changed to 0.5, so $k_1 = k_2 = k_3 = 0.5$. Each k value was now five times the original k value, so each reaction, and therefore the whole pathway as well, would be expected to happen more quickly. This can be seen in the result of the simulation in Figure 17 where the end behavior of the model occurs roughly five times sooner than when so $k_1 = k_2 = k_3 = 0.1$. Here, the initial concentrations were 14 mmol for 6-G-P and 28 mmol for NADP+. The curve for 6-P-G-delta-lactone and NADP+ reached asymptote around 30 seconds in the original simulation with these initial conditions, whereas they reached asymptote around 6 seconds below. The time to end behavior decreased by roughly a factor of five, which made sense since the reaction rates were each increased by a factor of five.

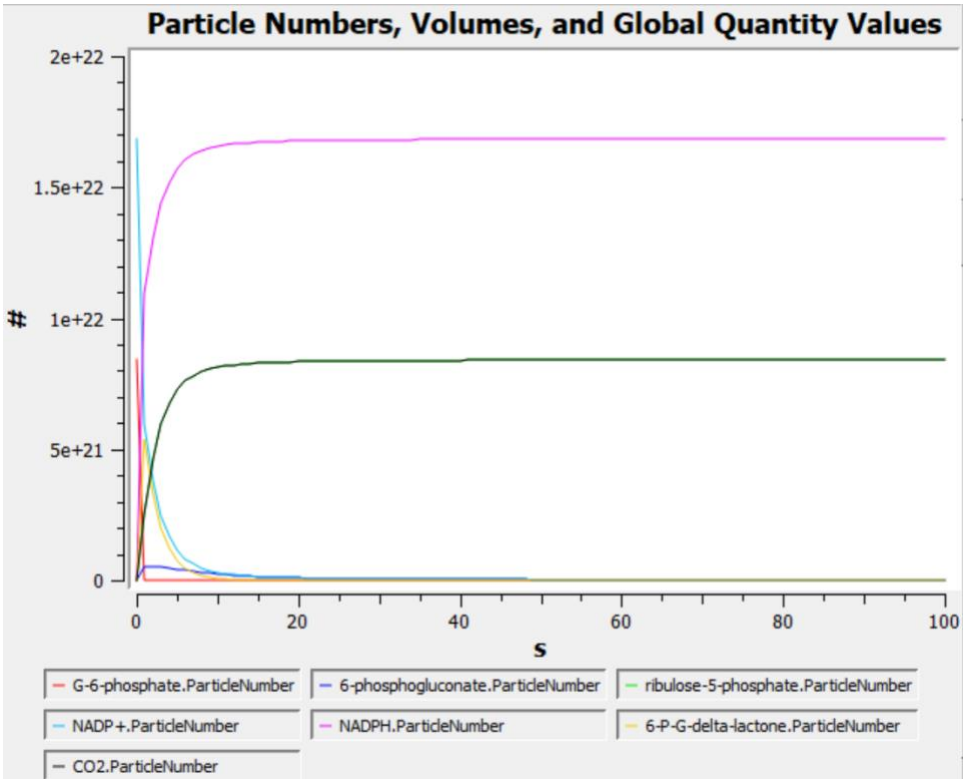

Figure 17. Copasi Time Course Simulation with Uniform k Value Increase and Initial Concentration of 14 mmol.

An additional simulation varying the k value uniformly for each reaction was performed by changing each k value to 0.05. Figure 18 shows the same initial conditions for $k_1 = k_2 = k_3 = 0.05$, each of which is half the original k value for each reaction. Therefore, the end behavior of the model took twice as long to occur, as seen here by the asymptotically trending 6-P-G-delta-lactone and NADP+ curves at around 60 seconds, rather than their original 30 seconds. From these two simulations, it is likely that uniformly changing the k value increases or decreases the overall pathway reaction time uniformly.

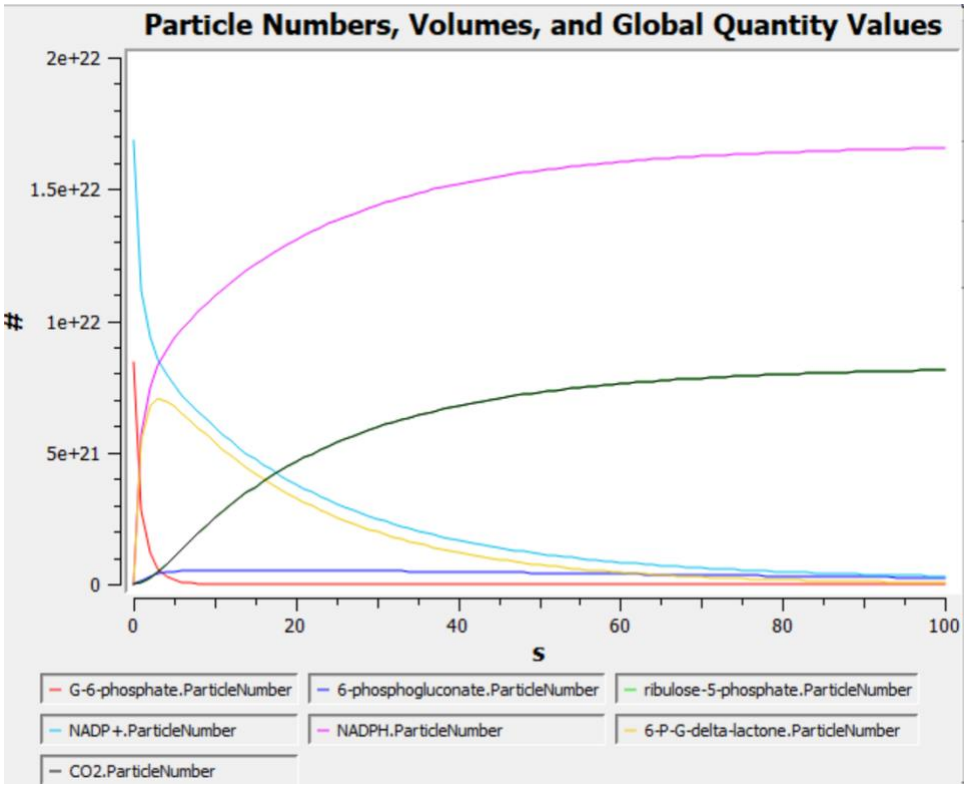

Figure 18. Copasi Time Course Simulation with Uniform k Value Decrease and Initial Concentration of 14 mmol.

However, changing the k values non-uniformly had different effects. Changing k_1=0.5 while k_2 = 0.1 and k_3 = 0.1 resulted in Figure 19. Here, the amount of G-6-P dropped almost immediately along with the amount of NADP+ since the first reaction was so much faster than the others. The amount of NADPH also increased sharply due to this reaction being faster. The other curves remained approximately the same since their reactions were untouched.

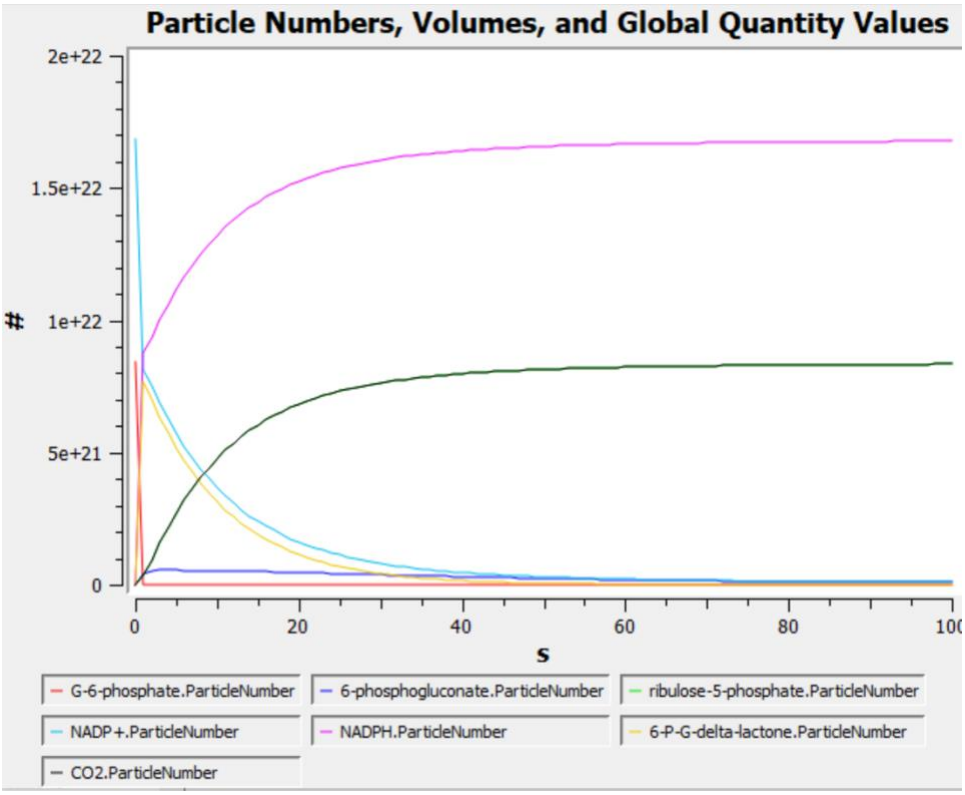

Figure 19. Copasi Time Course Simulation with k1=0.5 and Initial Concentration of 14 mmol.

Running $k_1 = 0.1$, $k_2 = 0.5$, and $k_3 = 0.1$ resulted in Figure 20. Here, the reaction rate of 6-P-G-delta-lactone to 6-phosphogluconate was increased, so the yellow curve of 6-P-G-delta-lactone decreased more steeply, and the dark blue curve of 6-phosphogluconate had a higher and sooner peak as more 6-phosphogluconate was produced sooner from that increased reaction rate. The peaks of NADPH, CO2, and ribulose-5-phosphate (same curve as CO2) all occurred earlier, and the decrease in NADP+ was also earlier in the reaction. These would have also been a result of the second reaction happening faster and producing more product for those reactions earlier in time.

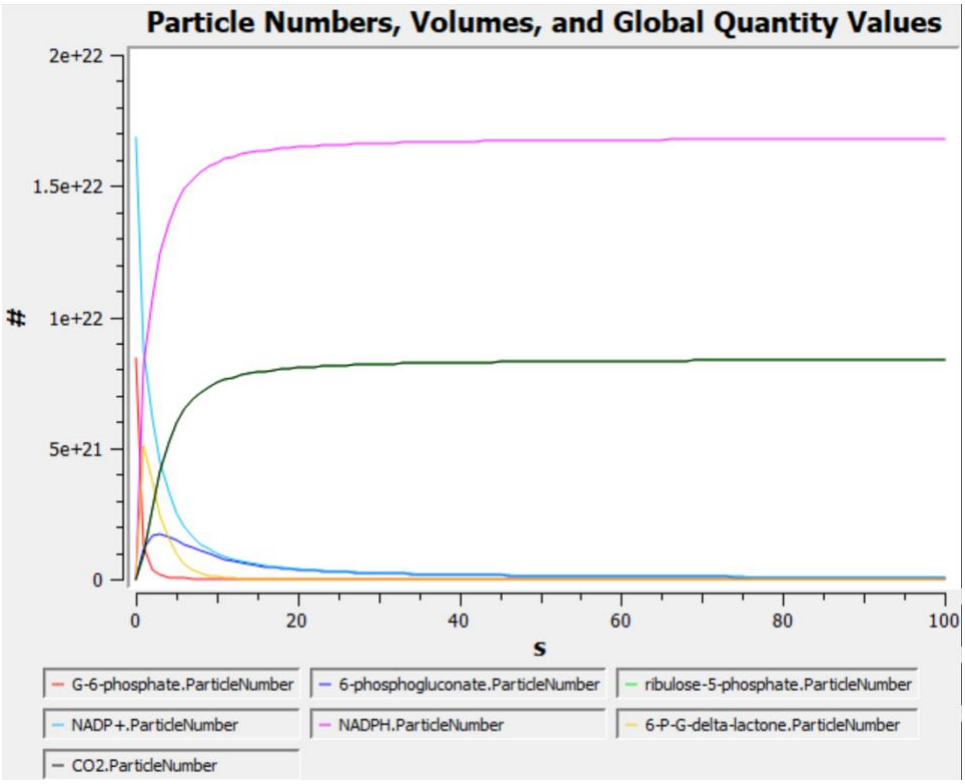

Figure 20. Copasi Time Course Simulation with k2=0.5 and Initial Concentration of 14 mmol.

Running $k_1 = 0.1$, $k_2 = 0.1$, and $k_3 = 0.5$ resulted in Figure 21. This plot looks nearly identical to the original 14 mmol plot. The slight differences are that the 6-phosphogluconate and the G-6-P curves align at the bottom and the NADP+ and 6-G-P-delta-lactone curves align in the curve portion. Possibly, the NADP+ (light blue) decrease occurred slightly more steeply since the third reaction was increased in speed, causing the curve to drop and align with the 6-G-P-delta-lactone (yellow) curve. The 6-phosphogluconate curve dropping is harder to explain, but perhaps the CO2 curve is steeper in this reaction since the product was created more quickly, thereby causing the 6-phosphogluconate curve to look less steep and closer to the G-6-P curve.

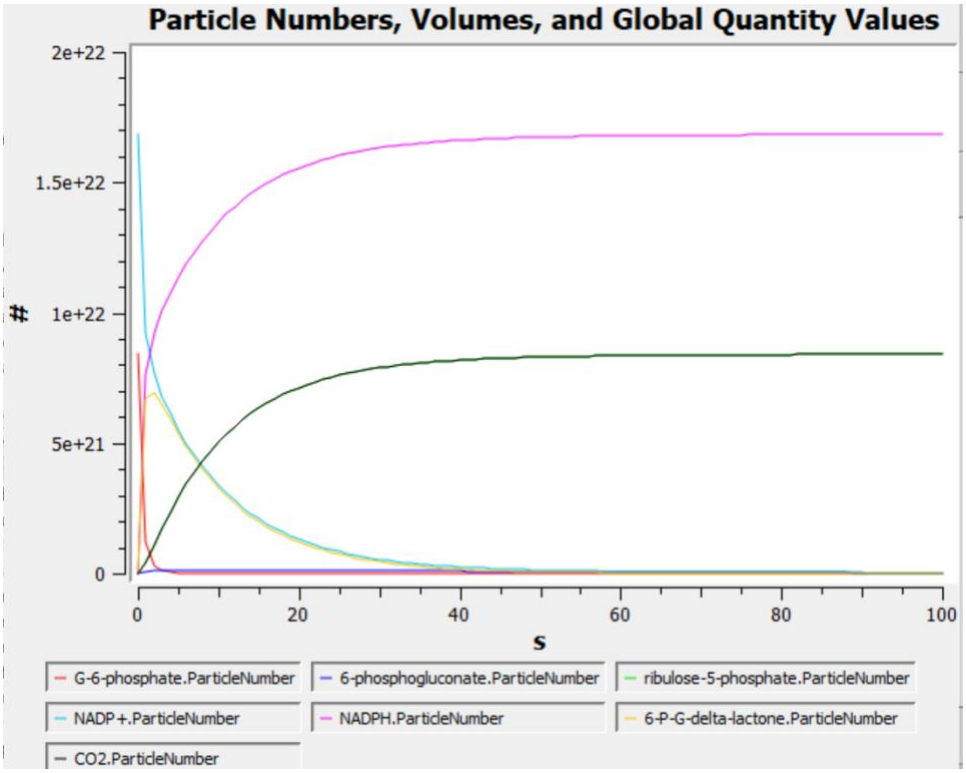

Figure 21. Copasi Time Course Simulation with k3=0.5 and Initial Concentration of 14 mmol.

Finally, another simulation was run in which all three k values were different. The plot in Figure 22 resulted from $k_1 = 0.05$, $k_2 = 0.5$, and $k_3 = 0.2$, with G-6-P initial concentration of 14 mmol. The overall shape of the curves is similar to the original model with all k values equal to 0.1, but the location of the peak or trough of each curve varied due to the different k values. The decrease of G-6-phosphate occurred more slowly since the first reaction was slower. The peak of the CO2, ribulose-5-phosphate, and NADPH curves all occurred earlier since the third reaction occurred more quickly. The 6-P-G-delta-lactone decreased much more quickly since it was a reactant in the second reaction, which occurred much more quickly in this simulation.

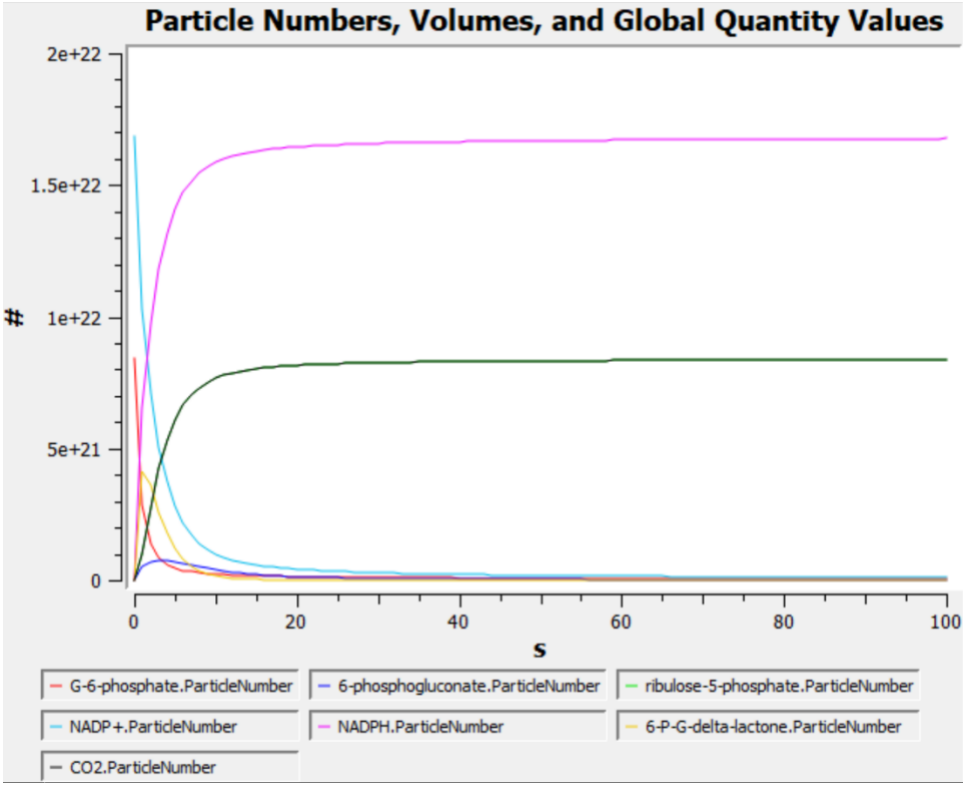

Figure 22. Copasi Time Course Simulation with k1=0.05, k2=0.5, k3=0.2 and Initial Concentration of 14 mmol.

Step 9: Predictions for the model

Once we had refined our model (Step 7) and analyzed these changes (Step 8) to fully understand our model, we were able to predict certain scenarios that the pathway was likely to experience. We incorporated our pathways' enzymes into the model and decided to predict potential overexpression. We found an article by Lin Jin and Yanhong Zhou, 2019 which discusses how in human cell lines "elevated expression of G6PD [the first enzyme in the human pentose phosphate pathway] is predictive of poor survival of patients with cancer, indicating that G6PD may serve a vital role in tumorigenesis."[xxvii] This observation relates to human cells rather than *C. elegans*, but it nonetheless provided us with motivation to model an overexpression of G6P1DH, the first enzyme in the *C. elegans* pentose phosphate pathway.

We theorized that the overexpression of an enzyme would result in the reaction speed occurring at that point (the corresponding v_x equation) being multiplied by a factor. In other words, we predicted that an overexpression would mean the first reaction happens faster or more frequently than the other reactions. Our theory is that this would result in a sharper decrease in the initial reactant, G-6-P, and possibly a buildup of the product of the first reaction: 6-P-G-delta-lactone. We simulated this overexpression in step 10 to see if our prediction was correct.

Step 10: Compare predictions and experimental results

To test our theory of overexpression, we tried using the same conditions as our original model (with 2 mol NADP+) but changed k_1 from 0.1 to 0.5 to attempt to simulate an overexpression of the first enzyme G6P1DH. The results below demonstrate the same general trends, but G-6-P declined significantly while 6-P-G-delta-lactone and 6-phosphogluconate peaked more strongly and more quickly than in the previous simulations. The G-6-P sharp drop fit with our prediction, and logically made sense. Since the enzyme of the first reaction was overexpressed, the reaction happened faster or more frequently, and therefore the initial reactant was consumed faster, causing a sharp drop.

The higher and sooner peak in 6-P-G-delta-lactone also fit our prediction. This indicated a slight buildup of 6-P-G-delta-lactone where 6-P-6-delta-lactone was made quickly by the first reaction, but the second reaction could not keep up with this pace. Therefore, a higher peak was created, and this peak happened sooner since the first reaction happened faster.

The unexpected portion of the result was the higher and sooner peak of 6-phosphogluconate, which we did not predict. A possible explanation was that the reaction creating 6-phosphogluconate was able to occur earlier in time as a result of the 6-P-G-delta-lactone being created earlier due to the first reaction increasing in speed. Since it occurred earlier in time, the peak occurred earlier. The peak could also have been higher due to the higher peak in the 6-P-G-delta-lactone. More 6-P-G-delta-lactone being produced earlier in the simulation would result in more 6-phosphogluconate also being produced earlier in the simulation, explaining this higher and sooner peak.

In addition, the increase in NADPH and the decrease in NADP+ were also shifted forward slightly in time, which we did not predict. This shift also made sense since the first reaction involved the conversion of NADP+ to NADPH, which would happen more quickly since the first reaction increased in speed.

The graph in Figure 23 is modeled after parameters $k_1 = 0.5$, $k_2 = 0.1$, $k_3 = 0.1$, with 2 mol initial NADP+ and 1 mol initial G-6-P.

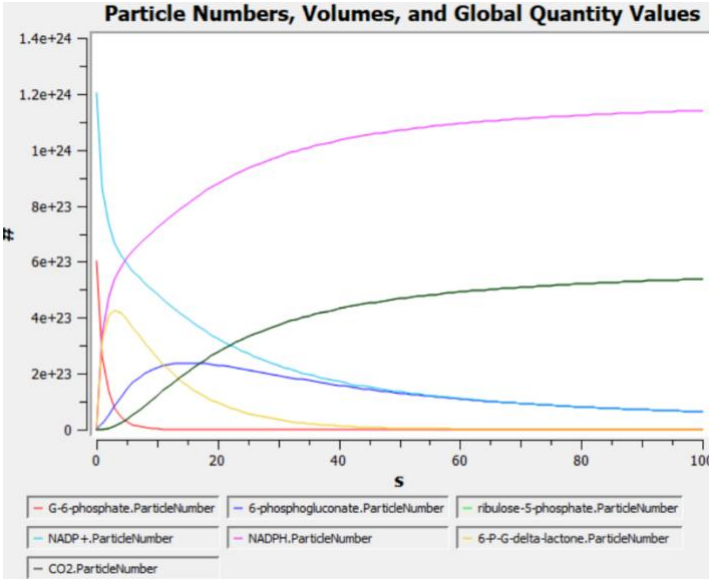

Figure 23. Copasi Overexpression Time Course Simulation

DISCUSSION

The primary strength of the pentose phosphate pathway in *C. elegans* model we created comes from the fact that the pentose phosphate pathways in *C. elegans* and in humans are well documented and explored. We know with relative certainty that our substrates, reactions, and mathematical models are decently accurate. Given this strong baseline, varying stochastic vs. deterministic methods, Mass Action vs. Michaelis-Menten kinetic laws, and the values for k_m, v_{max}, and k_1 as we did across time course simulations was likely to yield accurate general trends in the effects produced by such changes. While these general *trends* may be somewhat accurate due to the strong baseline of our model, the actual values produced by running time course simulations were almost certainly imprecise and inaccurate. This is primarily because, in setting a 1:1 reaction, we assumed that 100% of the glucose entering this pathway went toward this one reaction—in other words, we presumed no comingling with other pathways—which is not a reasonable assumption.

In testing our model, we also found many unexpected results. We were able to refine the model and account for some such results, as discussed in detail in the Approach & Methods section and summarized in the Conclusion section. However, other unexpected results were never explained. Namely, we were never able to correct the delayed addition of NADP+ in Reaction 3 in Copasi or in CellDesigner. We know this to be a limitation of the software or our skills or both, and it has hence bled into being a limitation of our model. Additionally, we were never able to figure out why none of 6-P-G-delta-lactone, Ribulose-5-phosphate, or CO2 did not reach 14 mmol concentration. It is possible that there is a flaw in our model, that Copasi and CellDesigner account for the imperfect results of a perfect 1:1 ratio in the real world, that we are incorrectly predicting results of a correct model, or some combination of these!

The fact that we were unable to find an acceptable theory as to why 6-P-G-delta-lactone, Ribulose-5-phosphate, and CO2 did not reach their expected peak concentrations (though attempts are explained in depth under Figure 13 in Step 7) presents an exciting opportunity for discovery in of itself. Why does this happen? Is the model wrong or are we wrong in our interpretation?

Answering these questions would make the model more accurate for other discovery-based scientific queries which one may use this model today to answer. For example, one may use our

model to answer: how would the pentose phosphate pathway in *C. elegans* react to large random perturbations? How would the pentose phosphate pathway in *C. elegans* react to sudden increases or complete lack of incoming substrate? Answering each of these questions further answers the related question, how *might* the pentose phosphate pathway react in humans?

CONCLUSION

We decided to use a network-based deterministic continuous dynamic quantitative model of ordinary differential equations to measure substrate concentrations in the *C. elegans* pentose phosphate pathway over time. To employ this model, we made critical assumptions about the initial reaction rates, the initial concentrations (within an acceptable range), as well as the assumption that 100% of the glucose entering this pathway goes toward this one reaction. Essentially, we're presuming no interconnecting pathways.

We first tried Mass Action kinetic laws with both stochastic and deterministic models in Copasi. The stochastic method resulted in constant concentrations over time which validated our original thinking that this model should not be used. The deterministic model had expected results: G-6-P decreased in concentration, NADP+ was exhausted, NADPH was made in Reaction 1, NADPH at the end of the pathway had concentration amount 2, 6-P-G-delta-lactone was made and then decreased, 6-phosphogluconate was made, Ribulose-5-phosphate and CO2 had the same curve AKA they were made in the same 1:1 ratio of the same reaction. The deterministic model also had some unexpected results: G-6-P did not reduce to 0 mol, NADPH was not made in Reaction 3 nor did NADP+ reflect the reactions where additional NADP+ was added during Reaction 3, 6-P-G-delta-lactone did not reach 14 mmol, 6-phosphogluconate was not consumed, Ribulose-5-phosphate and CO2 did not reach 14 mmol concentration.

The fact that NADP+ and NADPH did not reflect the reactions where additional NADP+ was added during Reaction 3 was likely a result of a known limitation of Copasi wherein species cannot be added on a delay.

We reasoned that this limitation could be accounted for by switching to CellDesigner and possibly by switching from Mass Action Kinetics to Michaelis-Menten kinetics. We made these changes respectively but were only able to account for the delay in glucose-related species rather than NADP+. Hence, the NADP-related species remained unchanged. Further, switching kinetic rate laws yielded no change to any of the expected nor unexpected results, except for the fact that the reaction occurred more quickly (due to our higher input kinetic rates) and now 6-phospholuconate was consumed! One additional unexpected result occurred however: the amounts of 6-phosphoglucono-delta-lactone and 6-phosphogluconate did not reach 14 mmol. Perhaps

CellDesigner accounts for an imperfect system when using small concentration amounts such as these.

We tried another method to correct the fact that NADP+ and NADPH did not reflect the reactions where additional NADP+ was added during Reaction 3 in Copasi. This time, we doubled the initial concentration of NADP+, hoping that the simulation would send one mol through Reaction 1 and one mole through Reaction 3. This attempt was unsurprisingly futile, and we decided to refocus our attention toward unexpected results.

Next, we tried to account for the fact that many of the decreasing substrates did not reach 0. This time, we ran the time course 10x longer than previously, and found that the substrates did indeed reach 0 over time and 6-phospholuconate was consumed, so the latter was not due to the change in kinetic rate laws after all.

In varying the kinetic rate variables as well as substrate concentrations, we found that end behavior trends remain constant so long as the ratio of kinetic rate to initial concentration of NADP+ does not allow NADP+ to go into negatives after 2 mol are consumed.

Now that we had tested, refined, and analyzed our model to a point we deemed acceptable, we decided to make a prediction about overexpression of the first enzyme and test it. We predicted that an overexpression would mean the first reaction happens faster or more frequently than the other reactions, resulting in a sharper decrease in the initial reactant G-6-P and possibly a buildup of the product of the first reaction, 6-P-G-delta-lactone. Simulating this overexpression found that G-6-P dropped sharply, and 6-P-G-delta-lactone peaked higher and sooner than in the previous simulations, as expected. Unexpectedly, 6-phosphogluconate also peaked higher and sooner than in the previous simulations, and also, NADPH increased and NADP+ decreased sooner. The first unexpected result likely happened as a direct result of 6-P-G-delta-lactone since they are directly related. The second likely happened because the first reaction involved the conversion of NADP+ to NADPH, which occurred more quickly as a result of the over-expression. This hypothesis-testing proved a perfect example of scientists (us) being technically correct but incompletely so until we prove so experimentally!

INDIVIDUAL CONTRIBUTIONS

Nikki Tirrell contributed to Step 1 ‘Choosing the Model’ and Step 2 ‘Literature Review’ as well as performed and wrote Step 3 ‘Visualize the Model’, Step 5 ‘Form a Mathematical Method’, and Step 6 ‘Test the Model’, contributed to Step 7 ‘Refine the Model’, and added explanation/questions throughout each section.

Casey Grage wrote the Abstract and Background, contributed to Step 1 ‘Choosing the Model’ and Step 2 ‘Literature Review’, wrote Step 4 ‘Conceptualize the Model’, wrote the Discussion, Conclusion, and References, proofread the final report, and added explanation/questions throughout each section.

Libby Lewis contributed to Step 2 ‘Literature Review’ and Step 7 ‘Refine the Model’, performed Step 8 ‘Analyze the System’, wrote Step 9 ‘Predictions for the Model’ and Step 10 'Compare Predictions and Results’, created the Petri nets in the Supplemental Material, and added explanation/questions throughout each section.

SUPPLEMENTARY MATERIALS

In examining our options for a model, we considered using a Petri net at one point. While we were successful in modeling the pentose phosphate pathway through a Petri net, we ultimately decided that modeling using differential equations would provide a more robust, thorough, and flexible model for experimentation, as discussed in Step 4 of our approach. We have chosen to include the Petri net model in the supplemental materials section to provide another angle at modeling the pentose phosphate pathway.

Figure 24 shows the initial conditions for the Petri net. Each circle is a place which represents a reactant, a product, or an enzyme in the pathway. The dark black bars represent a transition which fires once the correct number of tokens in the input places are present. The arrows point toward the black bars for inputs and away from the black bars for outputs. Initially, there are 3 tokens of G-6-P, and 6 tokens of NADP+. Here the tokens for NADP+ are split evenly between the two NADP+ places, which is not entirely accurate to reality, but for the sake of the model and the time steps, the split is necessary. This is a limitation to reality of the Petri net, but the overall movement of tokens can still be seen through this model. In this case, all of the arc weights are 1 for this network since the stoichiometric coefficients are all 1 for this reaction.

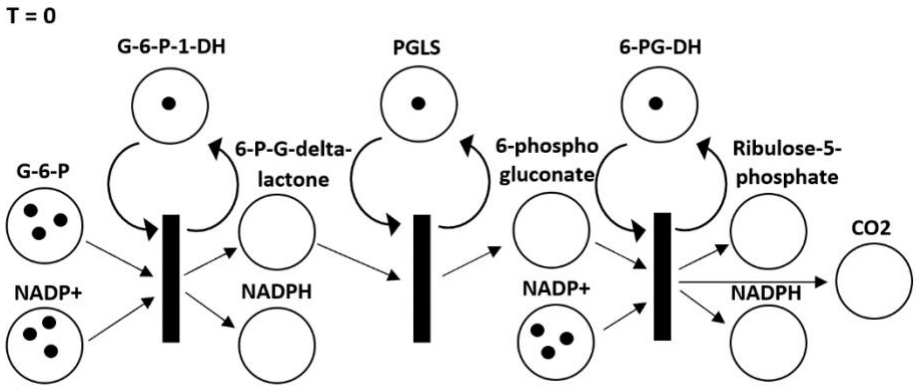

Figure 24. Initial State of Petri Net.

Since there is at least one token in G-6-P and one token in NADP+ and one token in G-6-P-1-DH, the first transition can fire. The result is shown in Figure 25. One token of 6-P-G-delta-lactone and one token of NADPH are produced while a token if G-6-P and a token of NADP+ are consumed. There is still one token for G-6-P-1-DH since this enzyme is not consumed in the reaction.

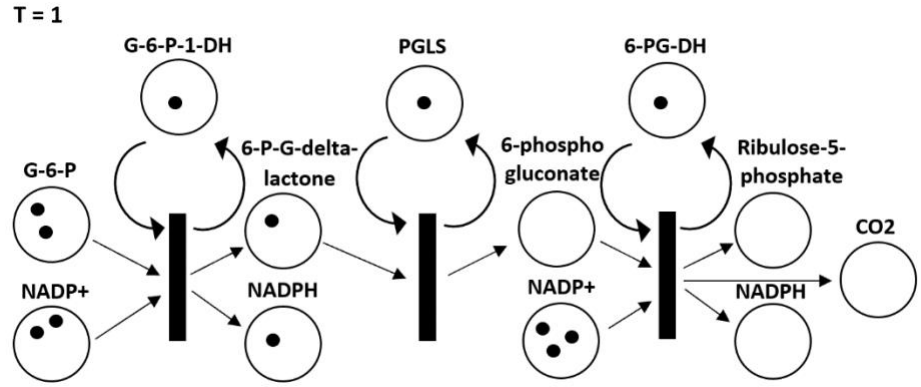

Figure 25. State of Petri Net After First Transition Fire.

After the next fire, the state of the Petri net is Figure 26. There were enough tokens for the first transition to fire and for the second transition to fire, so one token of 6-phosphogluconate, 6-P-G-delta-lactone, and NADPH each were created, while one token of G-6-P, NADP+, and 6-P-G-delta-lactone were consumed. PGLS is also not consumed in the reaction, so there is still one token of the enzyme left.

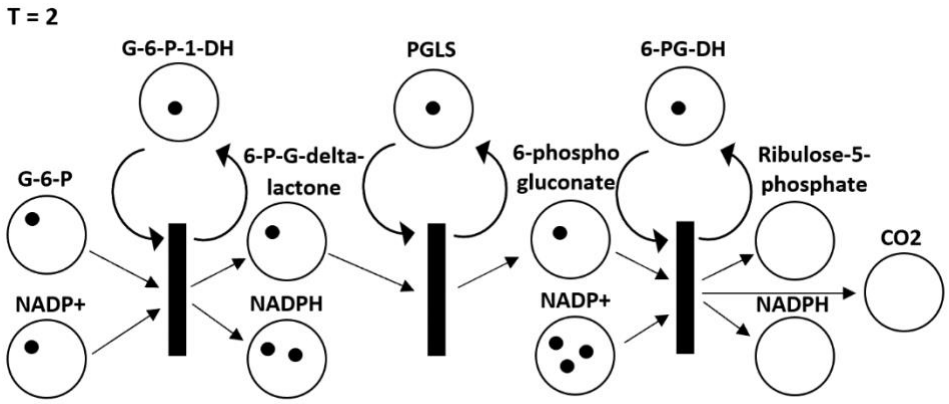

Figure 26. State of Petri Net After First and Second Transition Fire.

Next, there are enough tokens for the first, second, and third transitions to all fire, the result of which is shown in Figure 27. One token of ribulose-5-phosphate, CO2, 6-phosphogluconate, and 6-P-G-delta-lactone each are created. Two tokens of NADPH are created. One token of G-6-P, 6-P-G-delta-lactone, and 6-phosphogluconate are consumed. Two tokens of NADP+ are consumed. As like the other enzymes, 6-PG-DH is not consumed in the reaction, so one token still remains in its place.

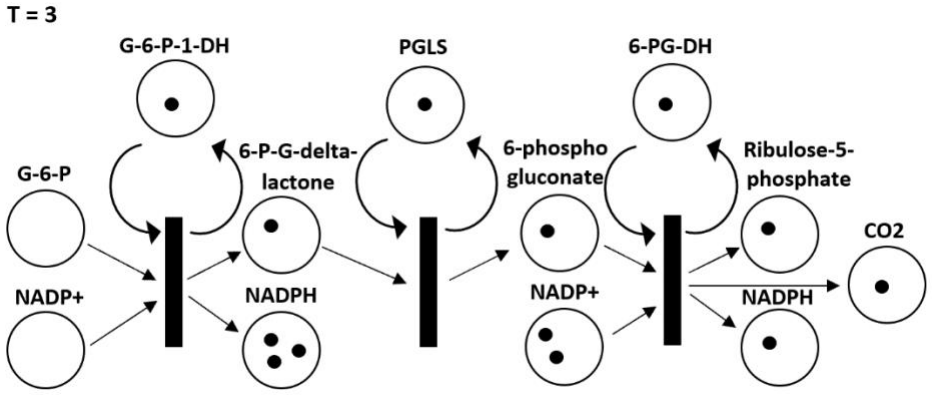

Figure 27. State of Petri Net After First, Second, and Third Transition Fire.

After this state, there are no more tokens in the G-6-P place, so the first transition can no longer fire. However, the second and third transition can each fire again, resulting in Figure 28. One token of 6-phosphogluconate, ribulose-5-phosphate, CO2, and NADPH each were created, while one token of 6-P-G-delta-lactone, 6-phosphogluconate, and NADP+ were consumed. The enzyme places each still have one token since the enzymes are not consumed in the reactions.

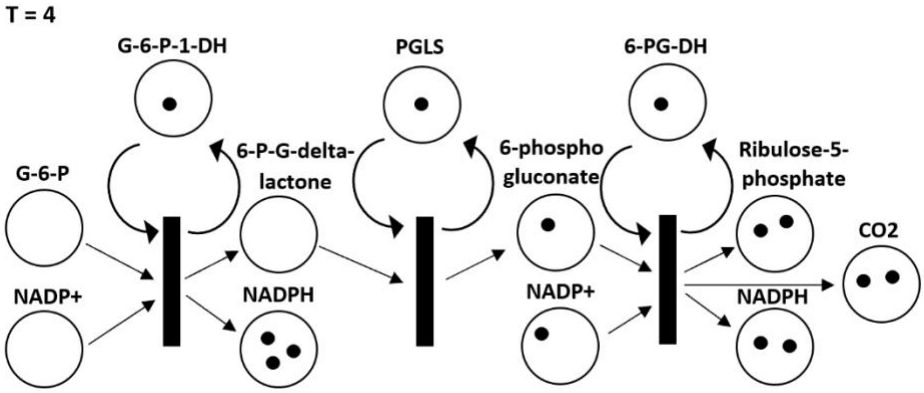

Figure 28. State of Petri Net After Second and Third Transition Fire.

At this point, the second transition can no longer fire since there are no tokens left in 6-P-G-delta-lactone. However, the third transition can fire one more time, consuming the final 6-phosphogluconate and NADP+ tokens to create a ribulose-5-phosphate, NADPH, and CO2 token, as seen in Figure 29. Again, the enzymes each still have one token since they are not consumed in the reactions.

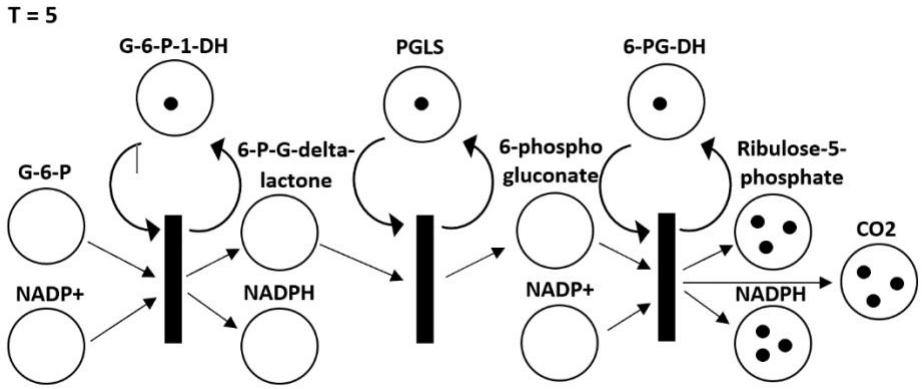

Figure 29. State of Petri Net After Third Transition Fire.

At this point, there are no more transitions that can fire since none of the input combinations have the correct number of tokens for firing. Therefore, this is the final state of the Petri net for these initial conditions. Many more simulations can be run with different initial conditions, such as tokens being present further down the pathway, but this simulation gives an overview of the pentose phosphate Petri net.

REFERENCES

[i] Ewbank, Jonathan. "Innate Immunity in C. Elegans." *CIML*, http://www.ciml.univ-mrs.fr/science/lab-jonathan-ewbank/experts.

[ii] White, J.G., Southgate, E., Thomson, J.N., and Brenner, S. (1986) The structure of the nervous system of the nematode *Caenorhabditis elegans*. *Philos. Trans. R. Soc. B*, 314 (1165), 1–340.

[iii] Jarrell, T.A., Wang, Y., Bloniarz, A.E., Brittin, C.A., Xu, M., Thomson, J.N. *et al.* (2012) The connectome of a decision-making neural network. *Science*, 337 (6093), 437–444.

[iv] C. elegans Sequencing Consortium (1998) Genome sequence of the nematode *C. elegans*: a platform for investigating biology. *Science*, 282, 2012–2018.

[v] Hillier, L.W., Coulson, A., Murray, J.I., Bao, Z., Sulston, J.E., and Waterston, R.H. (2005) Genomics in *C. elegans*: so many genes, such a little worm. *Genome Res.*, 15 (12), 1651–1660.

[vi] WormBase referential freeze WS210, Jan. 2010

[vii] Gerstein MB, Lu ZJ, Van Nostrand EL, Cheng C, Arshinoff BI, et al. Integrative Analysis of the Caenorhabditis elegans Genome by the modENCODE Project. Science 2010 [PMC free article] [PubMed] [Google Scholar]

[viii] Shaye DD, Greenwald I. OrthoList: a compendium of C. elegans genes with human orthologs. PLoS One. 2011;6(5):e20085. doi: 10.1371/journal.pone.0020085. Epub 2011 May 25. Erratum in: PLoS One. 2014;9(1). doi:10.1371/annotation/f5ffb738-a176-4a43-b0e0-249cdea45fe0. PMID: 21647448; PMCID: PMC3102077.

[ix] WormBase in 2022—data, processes, and tools for analyzing Caenorhabditis elegans. Paul Davis, Magdalena Zarowiecki, Valerio Arnaboldi, Andrés Becerra, Scott Cain, Juancarlos Chan, Wen J Chen, Jaehyoung Cho, Eduardo da Veiga Beltrame, Stavros Diamantakis, Sibyl Gao, Dionysis Grigoriadis, Christian A Grove, Todd W Harris, Ranjana Kishore, Tuan Le, Raymond Y N Lee, Manuel Luypaert, Hans-Michael Müller, Cecilia Nakamura, Paulo Nuin, Michael Paulini, Mark Quinton-Tulloch, Daniela Raciti, Faye H Rodgers, Matthew Russell, Gary Schindelman, Archana Singh, Tim Stickland,

Kimberly Van Auken, Qinghua Wang, Gary Williams, Adam J Wright, Karen Yook, Matt Berriman, Kevin L Howe, Tim Schedl, Lincoln Stein, Paul W Sternberg. Genetics, iyac003. www.wormbase.org

[x] WormBook, ed. The C. elegans Research Community, WormBook, doi/10.1895/wormbook.1.7.1, http://www.wormbook.org

[xi] C. Kenyon, The first long-lived mutants: discovery of the insulin/IGF-1 pathway for ageing Philos. Trans. R. Soc. Lond. Ser. B Biol. Sci., 366 (2011), pp. 9-16, 10.1098/rstb.2010.0276

[xii] Arwen W. Gao, Reuben L. Smith, Michel van Weeghel, Rashmi Kamble, Georges E. Janssens, Riekelt H. Houtkooper, Identification of key pathways and metabolic fingerprints of longevity in C. elegans, Experimental Gerontology, Volume 113, 2018, Pages 128-140, ISSN 0531-5565, https://doi.org/10.1016/j.exger.2018.10.003.

[xiii] https://www.wikipathways.org/

[xiv] https://www.wikipathways.org/index.php/Pathway:WP312

[xv] https://www.wikipathways.org/index.php/Pathway:WP5043

[xvi] Edda Klipp, Wolfram Liebermeister, Christoph Wierling and Axel Kowald, Systems Biology A Textbook, Chapter 1, 2016

[xvii] Edda Klipp, Wolfram Liebermeister, Christoph Wierling and Axel Kowald, Systems Biology, A Textbook Second Edition, Chapter 4, Wiley-VCH 2016.

[xviii] van den Heuvel S. The C. elegans cell cycle: overview of molecules and mechanisms. Methods Mol Biol. 2005;296:51-67. PMID: 15576926.

[xix] Genetics 14: 'C. Elegans methods workshop' or, 'Putting genes into path- ways' (cureffi.org), http://www.cureffi.org/2014/10/20/genetics-14/

[xx] Schleich, K., Lavrik, I.N. Mathematical modeling of apoptosis. *Cell Commun Signal* 11, 44 (2013). https://doi.org/10.1186/1478-811X-11-44. , https://biosignaling.biomedcentral.com/articles/10.1186/1478-811X-11-44

[xxi] Thomas Eissing, Holger Conzelmann, Ernst D. Gilles, Frank Allgöwer, Eric Bullinger, Peter Scheurich, Bistability Analyses of a Caspase Activation Model for Receptor-induced Apoptosis*, Journal of Biological Chemistry, Volume 279, Issue 35, 2004, Pages 36892-

36897, ISSN 0021-9258, https://doi.org/10.1074/jbc.M404893200. (https://www.sciencedirect.com/science/article/pii/S0021925820859419)

[xxii] Oct 6. In: WormBook: The Online Review of C. elegans Biology [Internet]. Pasadena (CA): WormBook; 2005-2018. Available from: https://www.ncbi.nlm.nih.gov/books/NBK19668/

[xxiii] https://www.wikipathways.org/index.php/Pathway:WP2829; Conradt B, Xue D; "Programmed cell death."; WormBook, 2005 PubMed Europe PMC Scholia; and Gumienny TL, Hengartner MO; "How the worm removes corpses: the nematode C. elegans as a model system to study engulfment."; Cell Death Differ, 2001 PubMed Europe PMC Scholia

[xxiv] Pathway Citation: Wright, A. (2022). Apoptosis. Reactome, 82, https://reactome.org/content/detail/R-CEL-109581 (Mon Oct 31 2022); Image Citation: Image Citation for Apoptosis. Reactome, 82, https://reactome.org/content/detail/R-CEL-109581 (Mon Oct 31 2022)

[xxv] Kanehisa Laboratories, Cel04215 Apoptosis – multiple species, *October 1, 2022*, KEGG. https://www.kegg.jp/entry/cel04215

[xxvi] Schlotterer A, Kukudov G, Bozorgmehr F, Hutter H, Du X, Oikonomou D, Ibrahim Y, Pfisterer F, Rabbani N, Thornalley P, Sayed A, Fleming T, Humpert P, Schwenger V, Zeier M, Hamann A, Stern D, Brownlee M, Bierhaus A, Nawroth P, Morcos M. C. elegans as model for the study of high glucose- mediated life span reduction. Diabetes. 2009 Nov;58(11):2450-6. doi: 10.2337/db09-0567. Epub 2009 Aug 12. PMID: 19675139; PMCID: PMC2768179. https://www.ncbi.nlm.nih.gov/pmc/articles/PMC2768179/

[xxvii] Lin Jin, Yanhong Zhou, "Crucial role of the pentose phosphate pathway in malignant tumors" (Review), Published online on: March 5, 2019 https://doi.org/10.3892/ol.2019.10112, Pages: 4213-4221